PERFORMANCE EVALUATION OF A MODIFIED RACE R2084 ATDMA ACCESS MECHANISM

by

LEWIS WAI MAN CHEN

B.A.Sc. (Electrical Engineering), University of British Columbia, Canada, 1995

A THESIS SUBMITTED IN PARTIAL FULFILLMENT OF

THE REQUIREMENTS FOR THE DEGREE OF

MASTER OF APPLIED SCIENCE

in

THE FACULTY OF GRADUATE STUDIES

DEPARTMENT OF ELECTRICAL AND COMPUTER ENGINEERING

We accept this thesis as conforming

to the required standard

THE UNIVERSITY OF BRITISH COLUMBIA

April 1998

In presenting this thesis in partial fulfilment of the requirements for an advanced degree at the University of British Columbia, I agree that the Library shall make it freely available for reference and study. I further agree that permission for extensive copying of this thesis for scholarly purposes may be granted by the head of my department or by his or her representatives. It is understood that copying or publication of this thesis for financial gain shall not be allowed without my written permission.

Department of Electrical & Computer Engineering.

The University of British Columbia
Vancouver, Canada

Date Apr. 27, 98.

Abstract

The telecommunications industry is experiencing an unprecedented demand for mobile communication services. It is expected that mobile subsribers will increasingly use multimedia services such as data, voice, and video applications.

In this thesis, we study the access mechanism (medium access control (MAC) protocol and bandwidth allocation strategy) used in the RACE R2084 Advanced Time Division Multiple Access (ATDMA) system which focuses on the development of a third generation cellular system known as the Universal Mobile Telecommunication System (UMTS). In particular, we propose improvements to the ATDMA access mechanism which allow the base station to dynamically assign bandwidth to voice and video services based on their activity levels. The performance of the modified access mechanism is evaluated using the access delay and packet dropping probability experienced by the voice and video services under varying traffic-load conditions. For video service, it is shown that the modified access mechanism can increase the ATDMA system capacity by as much as 45% when compared to the original access mechanism. In supporting voice and video traffic simultaneously, simulation results show that the modified access mechanism can increase the system capacity, in general, while satisfying the QoS requirements for both voice and video services.

Table of Contents

List of Tables

List of Figures

Acknowledgment

I wish to express my great appreciation to my research supervisor, Professor Cyril Leung, for his support, guidance and careful critiques throughout the course of this thesis. I also wish to express my appreciation to my colleagues for their kindness and consistent help throughout my study at UBC. This work was partially supported by NSERC grant OGP0001731.

Finally, my thanks go to my family and friends for their encouragement and support throughout my graduate study.

Chapter 1 Introduction

The demand for wireless communication services is increasing rapidly and cellular carriers are employing digital technology to increase radio channel capacity, to provide better reliability, and to offer a wider range of services to mobile users. At present, many successful cellular systems are designed based on the Time Division Multiple Access (TDMA) technology. For instance, TDMA is currently used in the European and North American second generation digital cellular systems such as GSM and IS-54. Furthermore, it is used in wireless personal communication systems such as the Digital European Cordless Telecommunications (DECT) and the Personal Handyphone System (PHS) [1].

The evolving digital cellular radio technology, together with the development of high performance portable computers with networking capabilities, have resulted in a new concept of ubiquitous accessibility for mobile users. Personal Communication Systems (PCS), based on wireless technology, will have to evolve towards supporting a wide range of applications including voice, video, data, and multimedia. In the future, it is expected that mobile users with hand-held audio-visual terminals will access multimedia services over networks without any geographical restriction. To this end, researchers are working on the integration of wireless networks and broadband networks such as B-ISDN. Such integration requires the development of third generation wireless communication systems with the following features [2]:

- System capacity improved by using microcells with coverage radii of less than a few hundred meters [3].

- Packet transmission and switching. This technique allows flexible bandwidth allocation for different services. Also, it allows efficient multiplexing of services from bursty data/ multimedia sources [4].
- A medium access control (MAC) protocol which is highly flexible and efficient to support future integrated services.
- A simple bandwidth management strategy to perform statistical multiplexing of many users on a common channel inside each cell.

This thesis focuses on the development of a new MAC protocol coupled with a bandwidth management strategy which allows the base station to dynamically assign channels to support voice and low-resolution video services together in a TDMA-based cellular environment.

1.1 Motivation

In early TDMA-based PCS proposals, it was assumed that voice services would dominate future communication scenarios. As a result, the TDMA frame structure was designed in such a way that one time-slot in a frame could support a voice channel. These early proposed MAC protocols and channel management strategies designed primarily for supporting voice service may not be appropriate for supporting multimedia services with different quality of service (QoS) requirements.

In order to support a wider range of communication services with different QoS specifications, a more flexible and intelligent channel access mechanism must be developed. First, the access mechanism must employ a new MAC protocol which allows different multimedia applications to transmit reservation packets to inform the base station of their requested QoS. Furthermore, a new resource management scheme is required to assign resources to different multimedia

applications in order to satisfy their respective QoS requirements. The resulting access mechanism must also show improved capacity by statistically multiplexing different services on a common channel inside each cell. This can be achieved by providing burst level rather than call level channel reservation to mobiles in such a way that, during low activity periods of a transmitting terminal, channels are released back to the base station and can be re-allocated to other cellular network users.

1.2 Objectives

In this thesis, we examine and propose improvements to the access mechanism used in the RACE R2084 Advanced Time Division Multiple Access (ATDMA) project which focuses on the development of a third generation mobile system known as the Universal Mobile Telecommunication System (UMTS) [5]. The RACE R2084 ATDMA project is centered on the study of the radio interface and is intended to develop a set of techniques that can improve the system capacity (by an order of magnitude) when compared to the existing TDMA systems, while at the same time, improving the quality and range of services. The access mechanism considered for ATDMA is a modification of the Packet Reservation Multiple Access (PRMA) known as PRMA++. In this thesis, the ATDMA access mechanism is further developed such that the base station can dynamically assign bandwidth to support voice and low-resolution video traffic on a demand basis. The main objectives are as follow:

- To illustrate the ATDMA access mechanism proposed in [5].
- To propose a modification of the ATDMA access mechanism and examine its performance in stastistically multiplex variable bit rate (VBR) low-resolution video traffic.

- To evaluate the performance of the proposed access mechanism when voice and low-resolution video services are supported together in the system.
- To evaluate the performance of the proposed access mechanism when voice and low-resolution video services are assigned with different priorities in accessing channels.

The performance of the proposed access mechanism is evaluated through the measure of packet dropping probabilities and access delays of voice and video services using a simulation-based method.

1.3 Outline of the Thesis

In Chapter 2, relevant background information on the access mechanism employed in the RACE R2084 ATDMA project is provided. In Chapter 3, the ATDMA access mechanism is modified so as to support low-resolution video traffic in real-time. In Chapter 4, the performance of the modified ATDMA access mechanism in supporting video traffic is evaluated through computer-simulations. Chapter 5 assesses the effectiveness of the modified ATDMA access mechanism in supporting a mixed traffic of voice and video services in the system. Furthermore, the effects of assigning different priorities to the voice and video services in accessing channels are studied. Chapter 6 gives a conclusion of this thesis.

Chapter 2 Access Mechanism for the RACE R2084 ATDMA Project.

The RACE R2084 ATDMA project is concerned with the investigation of advanced time division multiple access for the Universal Mobile Telecommunications System (UMTS). The objective of the project is to develop a set of techniques which utilizes the advantages provided by packet transmission and switching to improve the overall mobile system capacity when compared to the existing time-division multiple access systems. Furthermore, the quality and range of services provided by the new system developed must be improved [6]. This chapter provides a description of the RACE R2084 ATDMA project, specifically in its access mechanism, frame and burst structure, and system operation in supporting voice service.

2.1 Access Mechanism

The access mechanism considered for the ATDMA system is a modified version of Packet Reservation Multiple Access (PRMA) known as PRMA++. In PRMA++, two frequency channels, which are managed in a time division multiplexing (TDM) manner, are assigned to each microcell as the up-link and the down-link. Transmission time on each channel is divided into a sequence of frames, made up of a fixed number of time slots. Mobile stations in a microcell share a common channel (up-link) for transmitting their packetized information towards the base station. The base-station delivers information to the mobiles through broadcast transmission of packetized information on the down-link. On the up-link, three types of time slots exist which are the information slots (I-slots) the reservation slots (R-slots), and the fast-paging acknowledgment slots (FP_{ack}-slots). The I-slots and R-slots are used for carrying information bursts and access contention bursts transmitted from mobile terminals to the base station, respectively. The FP_{ack}-

slots allows the mobiles to send acknowledgment messages to the base stations after they successfully receive the paging messages on the down-link. On the downlink, besides the presence of I-slots, there are acknowledgment slots (A-slots) and fast-paging slots (FP-slots). The A-slots enable the base station to signal the reception of access-contention burst that was transmitted from the mobiles in the paired R-slots on the up-link. Moreover, the base station uses the A-slots to allocate free I-slots on the up-link to mobiles. The FP-slots are used to inform mobiles of the locations of the time slots that contains the information destined for them on the down-link. The functions of different types of time-slots described above will be illustrated in more detail in later sections. The TDMA frame structure is shown in figure 2.1.

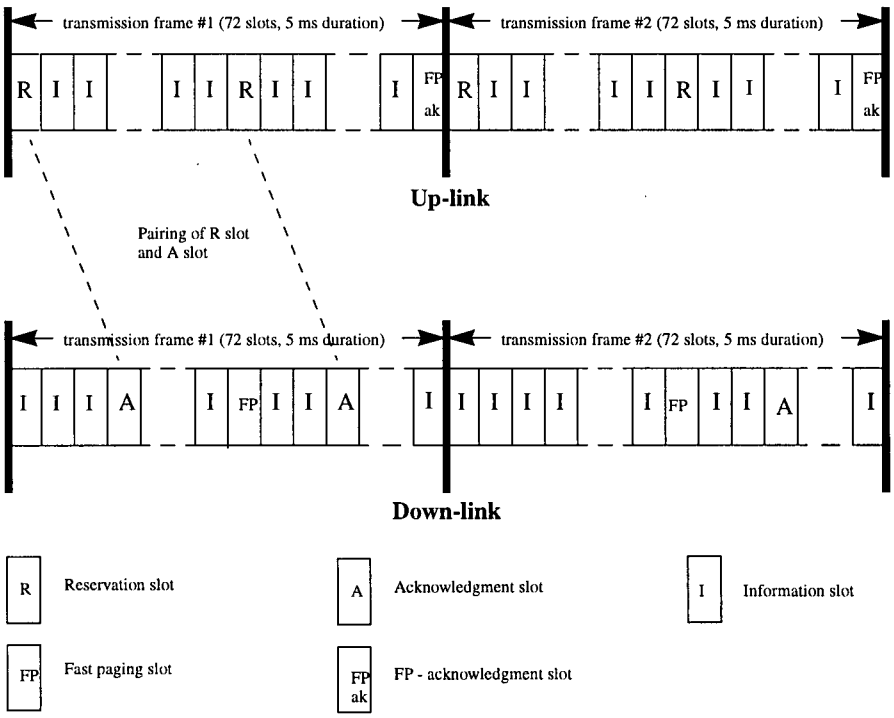

Figure 2.1. PRMA++ Transmission Frame Structure for a Microcellular Environment.

2.1.1 Channel Access

When a mobile becomes active, it transmits reservation request in the next available R-slot on the up-link. If free I-slot is available, the base station make I-slot assignment to the mobile in the paired A slot on the down-link. If no I-slot is available, the base station will send an acknowledgment message in the paired A-slot to inform the mobile to wait in the I-slot allocation queue. Mobiles waiting in the I-slot allocation queue will keep monitoring the A-slots on the down-link until they receive the I-slot assignments. With an I-slot assignment, the mobile gets uncontended use of the same I-slot in subsequent transmission frames until it has no information burst to send. To release the reserved I-slot back to the base station, the mobile piggybacks a message on the last information burst to inform the base station that the I-slot can be retrieved and re-allocated to other users in the next transmission frame.

When the base station has information bursts to deliver to the mobiles, the base station will signal the mobiles through the fast-paging (FP) slots on the down-link. Mobiles must listen to the FP-slots to receive the paging bursts. The paging bursts contain the addresses of the mobile terminals and the locations of the down-link I-slots in which they should receive the information bursts. After successfully receives the paging messages on the down-link, the mobiles will send acknowledgment messages to the base station using the FP_{ack} slots on the up-link.

2.1.2 Collision Resolution

When mobiles require I-slots for information bursts transmission, they need to reserve I-slots on the up-link by transmission of reservation requests in the R-slots. When more than one mobiles transmit reservation requests in the same R-slot, collision will occur and corrupt the reservation requests. Therefore, after transmitting a reservation request, a mobile must monitor

the paired A-slot on the down-link and assumed that the request has collided if it does not receive an acknowledgment message from the base station. A mobile having a collision will then back-off and retransmit in the next R-slot with a specified permission probability (P_r). The choice of the permission probability, P_r, may affect the performance of PRMA++. If P_r is too low, mobiles wait too long between successive transmissions; thereby increase the waiting time for mobiles to start transmissions in the I-slots. If P_r is too high, multiple collisions may be triggered which cause excessive delay due to the collision resolution process. In the ATDMA project, a P_r of 0.33 (uniform distribution) is chosen which means that an integer between 1 and 3 is assigned to a retransmitting mobile with equal probability. This integer assigned will then determine in which of the next three R-slots the mobile will attempt retransmission.

2.1.3 Contention and Packet Dropping

The statistical multiplexing gain obtained in PRMA++ derives from the fact that I-slots are allocated to mobiles only during their periods of activity and may be re-allocated to other terminals as soon as their activities cease. Therefore, the effectiveness of PRMA++ in granting channel access to mobiles depends on the fluctuating rates of information generated at the mobile terminals. When traffic builds up and the system becomes congested, the channel access delay experienced by mobiles will increase due to the increased number of reservation request collisions and the longer waiting time for mobiles staying in the I-slot allocation queue for free I-slot assignments.

Data sources which cannot tolerate information loss absorb the channel access delay as performance penalty. However, sources such as real-time video and speech, which require prompt information delivery and can tolerate some loss of information, simply discard delayed packets

[10]. For instance, packet loss of speech in PRMA++ occurs at the beginning of talkspurts. If a terminal drops the first packet of a talkspurt, it continues to contend for a reservation of I-slot to send the subsequent packets. This phenomenon is known as front-end clipping which impairs the quality of the received speech. The amount of front-end clipping is measured by the packet dropping probability, P_{drop}, which increases with the number of terminals being supported in the ATDMA system. A key measure of the performance of the ATDMA system in supporting voice traffic is the number of speech terminals that can be accommodated in the system within a given maximum value of P_{drop}.

2.1.4 A Comparison of PRMA++ and PRMA

In PRMA, all reservation requests must be transmitted to the base station in the I-slots; therefore, reservation requests will be blocked if all the I-slots have been allocated to mobiles. In contrast, PRMA++, which uses the control channels (R-slots and A slots) for the transmission and acknowledgment of reservation requests, can prevent the blocking of reservation requests when all I-slots are allocated. Furthermore, the presence of R and A-slots in PRMA++ can prevent occurrence of multiple collisions in accessing channels as in PRMA under high traffic-load conditions [8]. Also, a more reliable coding of information can be employed on the control channel than on the information channel in PRMA++. Thus, PRMA++ is more effective in providing protection against interference to the reservation requests when compared to PRMA [2]. This reliability of the control channel is essential for the successful communication between the base station and mobiles so that a flexible access mechanism can be implemented effectively. Lastly, unlike PRMA, PRMA++ allows the base station to have centralized control over the I-slot allocation policy. This feature enables the base station to prioritize the allocation of I-slots for

services with different quality of service (QoS) requirements [5].

2.2 Frame and Burst Structures

As shown in Figure 2.1, a transmission frame duration is 5 ms for the ATDMA system used in a microcellular environment. The following subsections introduces the structures of three types of transmission bursts: information burst, call-initialization burst and reservation burst.

2.2.1 Structure of Information (I) Burst

Mobiles transmit information as information bursts in the I-slots on the up-link. The structure of the information burst is shown in Figure 2.2. Each information burst can accommodate 66 information bits. Since a transmission frame has a duration of 5 ms, each I-slot can support a transmission rate of 13.2 kbit/s (i.e. $\frac{66 \text{ bits}}{5 \text{ ms}} = 13.2 \text{ kbits/s}$).

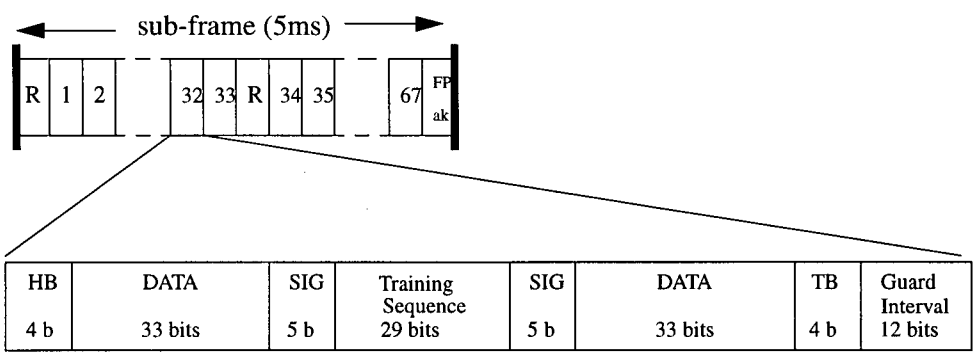

Figure 2.2. Structure of an Information Burst.

The signalling field (SIG) identifies the burst type as an information burst, or an information burst with in-band signalling, in which case the type of in-band signalling is also identified. In-band signalling is essential in supporting control processes of the ATDMA system such as link

measurement, automatic power control (APC), link adaptation, resource change requests, and automatic repeat request (ARQ) error protection. A detail description of these control processes can be found in [9]. A 3 bit flag is sufficient for signalling purposes which, after appropriate error control coding (1/3 rate) and adjustment for burst symmetry, amounts to 10 bits. The head (HB) and tail (TB) bit fields (each has a size of 4 bits) are used to indicate the beginning and end of the information burst. A guard time interval of 6μs (12bits) in duration is estimated to be sufficient for microcellular environment [6].

The components above amounts to a minimum transport burst size of (66 + 29 + 10 + 4 + 4 + 12) = 125 bits. For a 1.8 Mb/s carrier, a 5 ms frame duration can transport 9000 bits which would allow 72 time slots per transmission frame.

2.2.2 Structure of Call Set-up Initialization (CSI) Burst

Each mobile terminal has its own subscriber ID. When a terminal is switched on, it will request a mobile ID (for use in the cell) by transmitting its subscriber ID in a call set-up initialization (CSI) burst in the next available R-slot on the up-link. The base station will then check the subscriber ID for the authentication of the mobile terminal. If the terminal can be accepted into the cell, the base station will send a mobile ID to the voice terminal in the paired acknowledgment slot (A-slot) on the down-link. The structure of a CSI burst is shown in Figure 2.3.

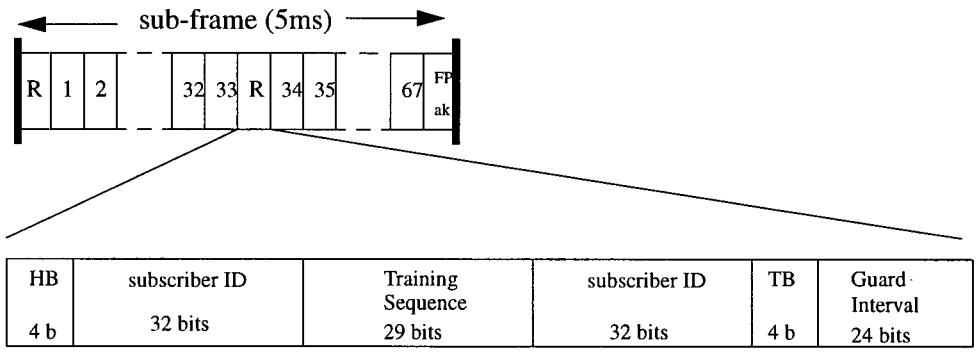

Figure 2.3. Structure of a Call Set-up Initialization Burst.

Since there is no adaptive frame alignment for the mobile before the call set-up initialization, a CSI burst must have a relatively larger guard time than the information burst. The overhead of a CSI burst consists of 4 head bits, 4 tail bits, and 29 bits training sequence. In addition to the overhead, the CSI burst contains a mobile ID of 32 bits. A half-rate coding is sufficient for the mobile ID since a loss of the CSI burst simply means that the mobile would not receive an acknowledgment from the base station and would retransmit again. After the channel coding, the burst overhead and the mobile ID occupy 101 bits. Therefore, a larger guard interval of 13.3μs (24 bits) is available for the CSI burst when compared to the information burst (6μs).

2.2.3 Structure of Reservation (R) Burst

When terminals become active from silence, they need to reserve I-slots for information bursts transmission by sending reservation bursts in the R-slots on the up-link. The structure of an access contention burst is shown in Figure 2.4.

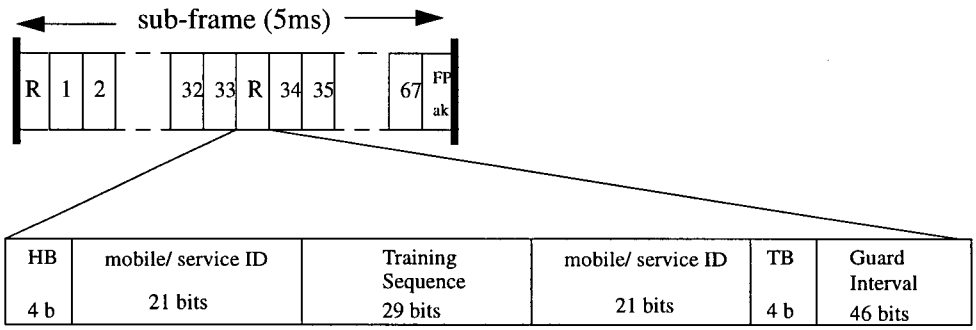

Figure 2.4. Structure of a Reservation Burst.

The overhead of a reservation burst consists of 4 head bits, 4 tail bits, and 29 bits of training sequence. Besides the overhead, the reservation burst consists of a mobile ID of 10 bits and a service identifier of 4 bits. The service identifier is to inform the base station of the types of traffic that the reservations are being made. The 4-bit service identifier allows for 16 possible service bit rates and is assumed to be adequate for future applications.

The accuracy of the information transmitted on the R-slots is essential for the successful operation of the PRMA++ access mechanism; thus, a more reliable coding such as rate one-third convolutional coding is used for the mobile service ID (which resulted in 14x3 bits = 42 bits after coding). A guard interval of 25.6μs (46 bits) is, therefore, available in a reservation burst.

2.3 System Operation and Performance Evaluation

In this section, the voice source model used in the ATDMA project is described. Next, the system operation of PRMA++ in supporting voice service and its performance is illustrated.

2.3.1 Voice Source Model

In voice service, the caller and callee do not speak continuously throughout the call duration. There are silence periods between speech segments when one or both parties do not speak. Statistical multiplexing of voice service in PRMA++ is achieved by using the silence periods to support other calls to increase the system capacity. It is assumed that a voice activity detector (VAD) can monitor the voice source and distinguish between talkspurt and silence intervals. Each talkspurt is encoded by a voice coder which produces individual blocks of duration 10 ms. The ATDMA frame structure has been developed to support a diagonal interleaving scheme of the voice coder with an interleaving depth of four. The diagonal interleaving scheme is illustrated in Figure 2.5.

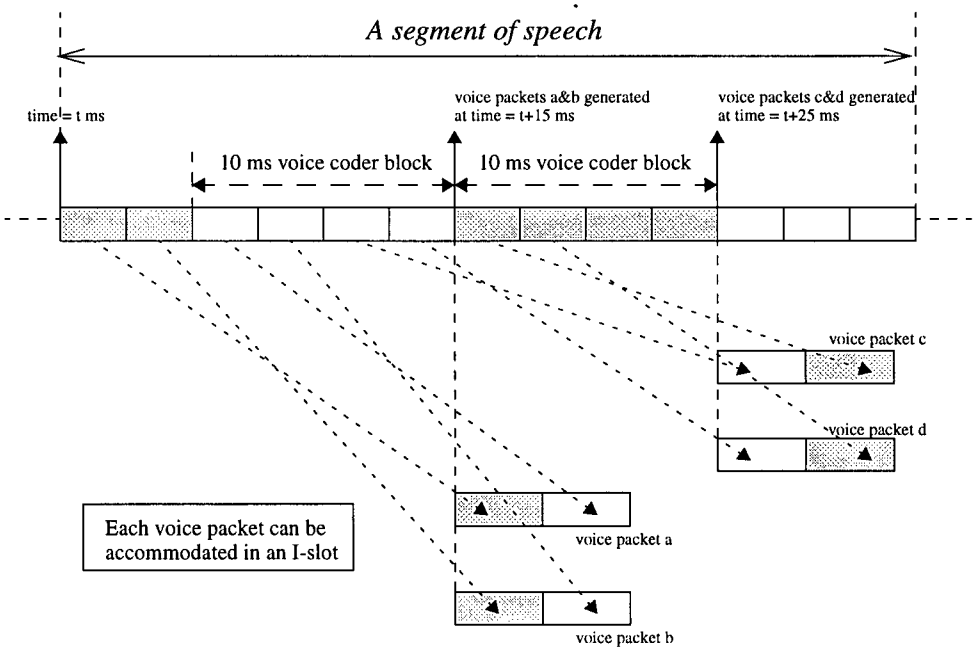

Figure 2.5. Diagonal Interleaving Scheme of Voice Coder.

In Figure 2.5, the voice coder codes each talkspurt into a number of blocks of 10 ms duration. Each coded voice-block is further divided into four sub-blocks which are then interleaved over four successive information bursts with the sub-blocks of the previous and subsequent 10 ms voice coder blocks. After interleaving, each information burst is called a voice packet which can be carried in an I-slot of the ATDMA system. At the receiver, a deinterleaver will re-arrange the interleaved sub-blocks carried in the voice packets in proper sequence and passes them to the speech decoder. Since the wireless channel exhibits bursty error characteristics, the process of interleaving and deinterleaving of the encoded speech increases the reliability in information transmission by spreading out the error bursts in time such that the errors appear to be more independent [11]. The VAD produces a mean talkspurt duration of 1.41s, and a mean silence duration of 1.74s. Therefore, a voice source has a speech activity ratio of approximately 44.8 percent (i.e. $\frac{1.41 \text{ sec}}{(1.41 + 1.74) \text{ sec}} \times 100\% = 44.8\%$).

2.3.2 System Operation

The flow diagram in Figure 2.6 shows the operation of the PRMA++ access mechanism in supporting voice service. At the start of a talkspurt, a mobile will attempt to reserve an I-slot by sending a reservation request in the first available R-slot on the up-link and monitor the paired A-slot on the down-link for an acknowledgment message. If no acknowledgment is received, the mobile will assume that collision has occurred and attempt retransmission with a given retransmission probability in the next available R-slot on the up-link. The time that elapses from the moment that a talkspurt begins to the instant that transmission starts in a reserved I-slot is defined as the access delay of voice service. A delay threshold of 10 ms is imposed for voice service so that voice packets will be dropped if they cannot be transmitted within 10 ms after their genera-

tion (the voice packet generation time is illustrated in Figure 2.5). When a voice packet is dropped due to excessive access delay, the mobile will continue to contend for I-slot reservation for the subsequent voice packets generated.

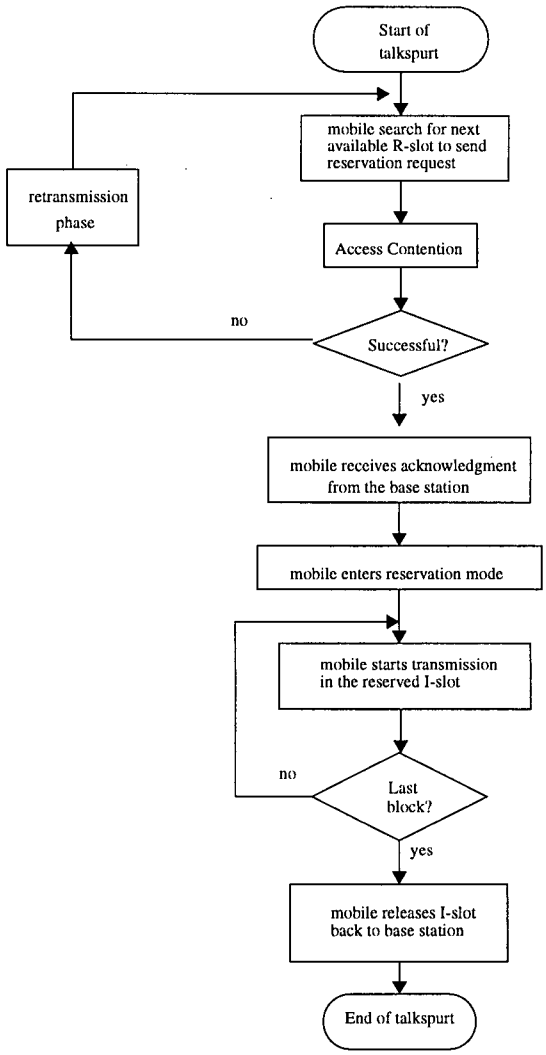

Figure 2.6. Operation of PRMA++ in Supporting Voice Service.

After successful transmission of a reservation request in the R-slot, the mobile will listen

to the paired A-slot on the down-link for I-slot assignment if free I-slot is available. If no I-slot is available, the base station will send an acknowledgment message in the A-slot and notify the mobile to wait in the I-slot allocation queue. While the mobile is waiting in queue, packet dropping commences if the waiting time exceeds the delay threshold of 10 ms. Packets will continue to be dropped until either an I-slot becomes available or all the packets in a talkspurt are lost and the mobile returns to the silence-state. Since the base station has centralized control of I-slot allocation, a prioritized allocation policy can be implemented when services with different priorities are mixed in the system.

Once an I-slot is successfully allocated, the mobile enters a reservation mode where the subsequent packets of a talkspurt are transmitted in the reserved I-slot in each transmission frame. On sending the last packet of a talkspurt, the mobile releases the I-slot back to the base station. The I-slot released is then available for other users in the next transmission frame. The above process is repeated for every talkspurt generated by a VAD.

The performance parameters associated with voice service are access delay and packet loss. A delay threshold of 10 ms is imposed in the following evaluation so that packets of a talkspurt will be dropped if they cannot be transmitted within 10 ms after their generation. Packet loss is derived from a counter which is incremented each time a voice packet is dropped due to violation of the 10 ms delay threshold.

2.3.3 Assignment of Priorities to the Acknowledgment Message and the I-slot Allocation Message for Voice Service

In PRMA++, the A-slots on the down-link need to carry two types of messages which are the acknowledgment message and the I-slot allocation message. In order for the PRMA++ to

function properly, appropriate priorities must be attached to the acknowledgment message and the I-slot allocation message whenever a conflict between them occurs. Figure 2.7 illustrates an example scenario which allows a study of the effects of assigning different priorities to the acknowledgment message and the I-slot allocation message when a conflict between them arises.

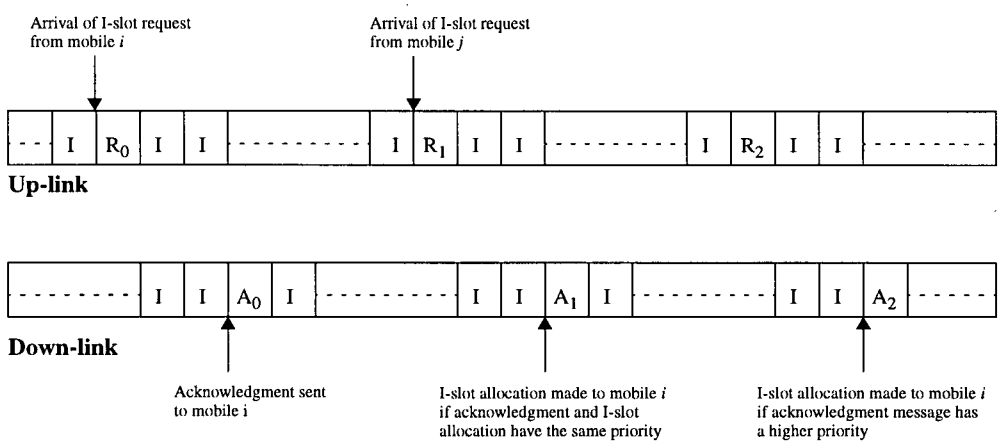

Figure 2.7. Assignment of Priorities to the Acknowledgment and the I-slot Allocation Message.

In Figure 2.7, voice terminal *j* sends a reservation request in the slot R_1. After transmission of the reservation request, terminal *j* will monitor the A-slot (A_1) on the down-link for the I-slot allocation message (if a free I-slot is available) or the acknowledgment message (if no I-slot is available). Assume that a mobile, *i*, is waiting in the I-slot allocation queue prior to the arrival of terminal *j* (mobile *i* sent I-slot request to base station in slot R_0) and that an I-slot is available at the beginning of the slot A_1. If there is no priority difference between the I-slot allocation message and the acknowledgment message, the base station, which serves the terminals on a first-come first-serve (FCFS) basis, will make an I-slot allocation to the terminal *i* in slot A_1 before

sending an acknowledgment message to the mobile *j*. Therefore, terminal *j* which does not receive an acknowledgment message will assume that the reservation request transmitted in slot R_1 was not successfully received by the base station. As a result, terminal *j* will mistakenly enter the collision resolution phase and re-send the reservation request in the next available R-slot (i.e. R_2) with a specified retransmission probability (as described in Section 2.1.2). However, when voice terminal *j* attempts a retransmission, it may collide with another reservation request(s) and cause the terminals involved to attempt more unnecessary retransmissions. This problem is more serious under high traffic load conditions in which there is larger number of mobiles waiting in the I-slot allocation queue for free I-slots. Under this condition, mobiles are less likely to be acknowledged on time after they sent reservation requests in the R-slots on the up-link. As a result, due to the delayed acknowledgment, more unnecessary retransmissions of reservation requests may occur which eventually leads to voice quality impairments caused by the excessive contention delay (i.e. delay in sending reservation request successfully in the R-slots).

The above problem is solved when the acknowledgment message is given a higher priority than the I-slot allocation message. Under this priority arrangement, the base station will first send an acknowledgment message to the voice terminal *j* in slot A_0 before making an I-slot assignment to the voice terminal *i*. As a result, the I-slot allocation made to the terminal *i* will be deferred to slot A_2 (if no further reservation request is received in the slot R_2). Although the video terminal *i* suffers an additional access delay, this priority arrangement can prevent mobile *j* from blocking other mobiles in accessing channel (i.e. sending reservation requests in R-slots) when terminal *j* attempt retransmission due to the delayed acknowledgment message. In all the simulation results presented in this thesis, a higher priority of the acknowledgment message over the I-slot alloca-

tion message is assumed.

2.3.4 Interference Issue

PRMA++ is different from the access schemes used in second-generation TDMA systems which allocate a time slot to a mobile for the duration of a call (assuming no handover). PRMA++ dynamically allocates time-slots to mobiles on a demand basis so that interference levels experienced by mobiles change more rapidly when compared to second generation TDMA systems. In PRMA++, there is an I-slot queue which allows the base station to assign I-slots to different users using different allocation policies. The ATDMA project has investigated the effects of using two I-slot allocation policies on the interference levels experienced by mobiles. These two policies are sequential slot allocation and random slot allocation policies. In sequential slot allocation policy, the base station will allocate the closest I-slot available to the mobiles waiting in the I-slot allocation queue. In random slot allocation policy, the base station randomly chooses an available I-slot within a transmission frame. Simulation results in [5] show that, when compared to the sequential slot allocation policy, the random slot allocation policy can reduce the mean interference level and yield approximately 1db gain in average carrier-to-interference ratio (C/I).

2.3.5 Performance Estimates

In this section, the performance of PRMA++ in supporting voice service is illustrated through results obtained by computer simulation. A simulation model is constructed, using Ptolemy [13], a discrete-event simulation tool, to implement the PRMA++ access mechanism. Table 2.1 shows a list of working values for the system parameters used in the simulation.

Table 2.1 Parameters Chosen for the PRMA++ Simulation Model.

Carrier bit rate	1.8 Mb/s
Speech coder rate	13 kb/s
Speech block length	10 ms
Packet dropping delay threshold	10 ms
Downlink acknowledgment delay	3 time-slots (208μ s)
Retransmission probability	0.33 (uniform distribution)
Transmission frame duration	5 ms (72 time-slots)
Speech activity factor	45%
Information (I) slots per transmission frame	56 to 70
Control slots per 5 ms transmission-frame	different no. of R-slots (paired with down-link A slots), 1 FP slot on the down-link paired with 1 FP_{ak} slot on the up-link.

Figure 2.8 shows the mean access delay for voice service when different numbers of R-slots are used in the system. The access delay is composed of the contention delay, acknowledgment delay and I-slot allocation delay. The contention delay is measured from the time that a talkspurt begins to the instant that a reservation request is successfully transmitted in an R-slot to the base station. After an acknowledgment delay of 3 time-slots duration, there is an I-slot allocation delay which measure the time that has elapsed after a mobile receives an acknowledgment from the base station to the instant that a transmission starts in the I-slot assigned. As the number of R-slots per transmission frame increases, mobiles can have more frequent access to the R-slots per transmission frame. Therefore, the waiting time for access-contention and the chance of having a collision are reduced. Hence, using more R-slots per transmission can decrease the contention delay which may lower the access delay. However, the number of R-slots per transmission frame can only be increased at the expense of reducing the number of I-slots. As a

result, using more R-slots per transmission frame may cause the mobiles to stay longer in the I-slot allocation queue for free I-slot assignments which may lead to an increase in the I-slot allocation delay.

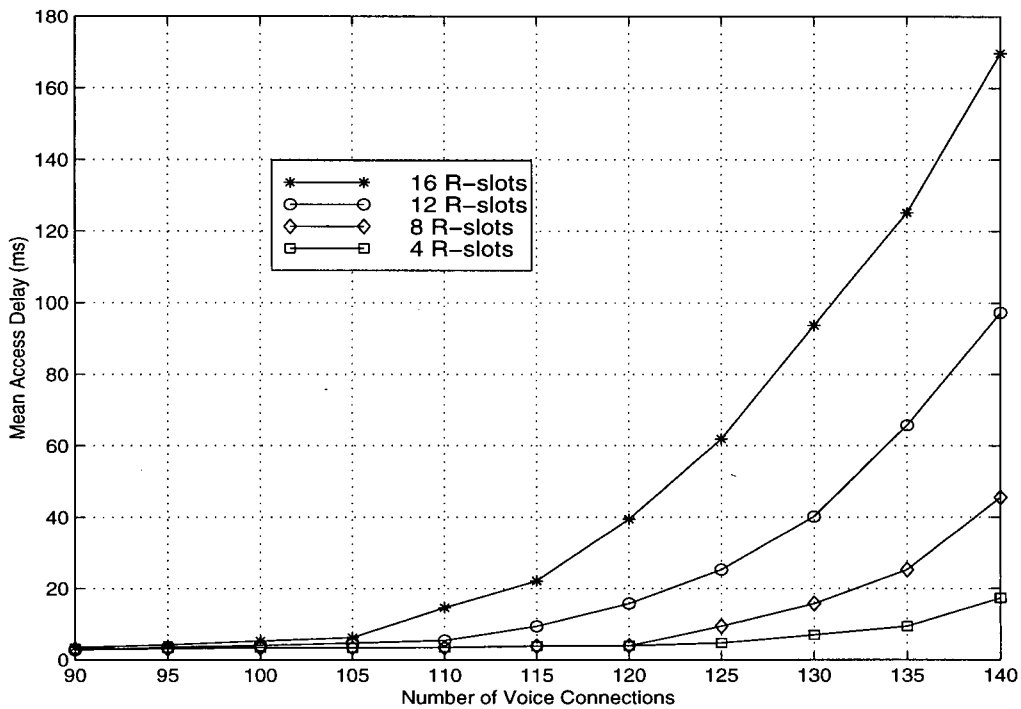

Figure 2.8. Mean Access of Mobiles Under Different Traffic-load Conditions.

As there are more voice connections established, Figure 2.8 shows that a system with more R-slots per TDMA frame has a faster rate of increase in access delay than a system with fewer R-slots. This observation indicates that as traffic load increases, the number of available I-slots decreases and more of the access delay experienced by mobiles are come from queueing for free I-slots. Hence, a system with fewer R-slots is more efficient in supporting mobiles under high traffic-load conditions [5]. However, as demonstrated in [5], when the number of R-slots is less than four per transmission frame, the system becomes unstable as traffic-load increases since

multiple collisions are triggered which cause excessive delay due to the collision resolution process. As a result, mobiles have difficulties in gaining successful access through R-slots and the system throughput drops significantly. For instance, when 3 R-slots are used per transmission frame, simulation in [5] shows that multiple collisions of reservation requests occur which causes excessive contention delay when the number of voice connections increases beyond 115. The excessive contention delay eventually leads to a significant quality degradation of voice traffic. Therefore, 4 R-slots per transmission per frame is chosen in the ATDMA project which can maximize the system while preventing the occurrence of multiple collisions of reservation requests under high traffic-load conditions [5].

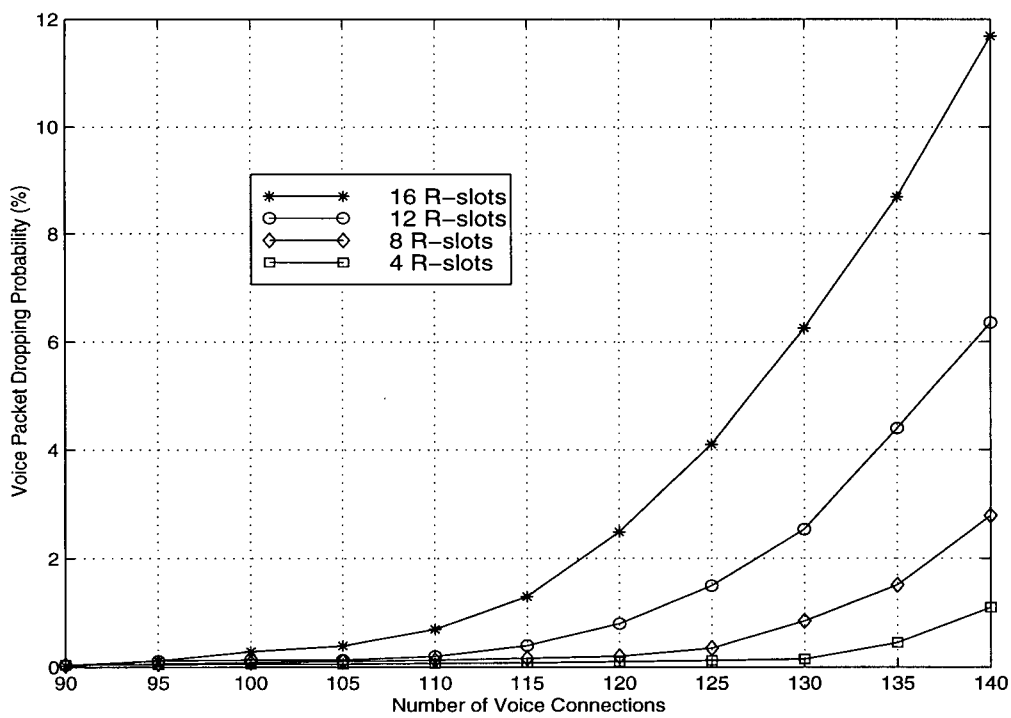

Figure 2.9. Voice Packet Dropping Probability Under Different Traffic-load Conditions.

Figure 2.9 shows the packet dropping probability for voice service under varying traffic-

load conditions when different number of R-slots are used in the system. The result shows that, as the traffic-load increases, the increasing access delay of voice traffic causes more voice packet to be dropped due to the violation of the 10 ms delay threshold. Therefore, the voice packet dropping probability rises accordingly. Furthermore, a system using more R-slots per transmission frame has a higher packet dropping probability when compared to a system using fewer number of R-slots. This result is expected because as traffic-load increases, system using more R-slots per transmission frame has fewer number of free I-slots. As a result, voice terminals need to wait longer in the I-slot allocation queue for free I-slots in those system using more R-slots per transmission frame. The maximum number of voice connections that can be supported in the ATDMA system without violating the 1% packet dropping probability threshold is 139 voice connections when 4 R-slots are used per transmission frame. Therefore, when PRMA++ access mechanism is used, a statistical multiplexing factor of 1.93 active voice users per time-slot can be achieved (i.e $\frac{139 \text{ users}}{72 \text{ slots}} = 1.93 \text{ users/ slot}$).

Chapter 3 Transmission of Low Resolution Video in the Modified ATDMA System

Advances in low bit-rate video coding technology, together with the development of digital cellular systems, have made possible the delivery of video services to mobile users through the bandwidth limited wireless network. In recent years, the telecommunication industry has shown growing interest in providing audio-visual services such as video telephony, video conferencing and video e-mailing in the wireless environment [4] [14]-[16]. In this chapter, several changes to the ATDMA access mechanism [5] are proposed such that low resolution video exhibiting variable bit-rate (VBR) characteristics can be supported. This chapter is divided into four sections. First, a low resolution video coding algorithm known as the H.261 codec is briefly described [17]. Next is a discussion of a modeling method to represent the output of the VBR H.261-based video codec using a stochastic model. Then, a packetization scheme which converts the coded bit-stream of the H.261-based codec into individual packets suitable for transmission in the ATDMA system is proposed. Finally, there is a detail description of modifications of the ATDMA access mechanism, which allows the base station to dynamically assign channels to video connections on a demand basis.

3.1 H.261 Video Codec

In order to accommodate growth of audio-visual services, the telecommunications industry has worked in standards for low bit rate video coding. Cooperation between the Motion Picture Expert's Group (MPEG, a joint committee of the International Standards Organization (ISO) and the International Electrotechnical Society (IEC)) and the International Telecommunications Union - Telecommunication Standardization Sector (ITU-T) led to the development of the

H.261 video codec in 1992[17]. The H.261 standard is designed for carrying the video component of audio-visual services such as videophone and video conferencing. H.261 has a bit-rate of less than p x 64 kbps, where "p" is an integer in the range of 1 to 30. For videophone applications which do not require high video quality, a "p" value of 1 or 2 can be used. The following subsections give an overview of the coding algorithm and the bit-stream structure of the H.261 codec. More details can be found in the H.261 Recommendation [17].

3.1.1 H.261 Coding Algorithm

The VBR video codec periodically generates a message, corresponding to the coded bit-stream of one video frame. The video frame rate of a video codec determines the number of generation periods (i.e. the number of video frame) per second. In the video sequences of audio-visual applications such as videophone, the video frames usually contain the background and a number of other objects which are essentially unchanged from one video frame to another. Some of the objects may only have slight movement such that their motions can easily be predicted from frame to frame. Most video codecs reduce the temporal redundancy of a video sequence by coding the difference between two consecutive video frames instead of coding the video frames independently. This technique is called inter-frame predictive coding. In contrast, the coding method which codes a video frame independently from others is called intra-frame coding. In reducing the spatial redundancy of a video frame, most video coding standards use discrete cosine transform (DCT) in video compression. In DCT transform, a matrix of inputs (e.g pixel values) is transformed into another matrix of output such that most of the information of the input matrix is extracted and contained in only a few elements of the output matrix [18]. Data compression can then be achieved on the transformed matrix by encoding and transmitting those elements that convey information.

H.261 uses a combination of inter-frame prediction and DCT coding to reduce the temporal and spatial redundancy of video frames, respectively. In H.261, the image of a video frame is first divided into a number of blocks known as a group of blocks (GOB). The number of GOBs in a video frame depends on the picture format chosen by the H.261 codec. Each GOB in turn, consists of 33 macroblocks (MB) as shown in Figure 3.1 [19]. Inter-frame coding of H.261 is implemented at the MB level known as block-based motion compensation.

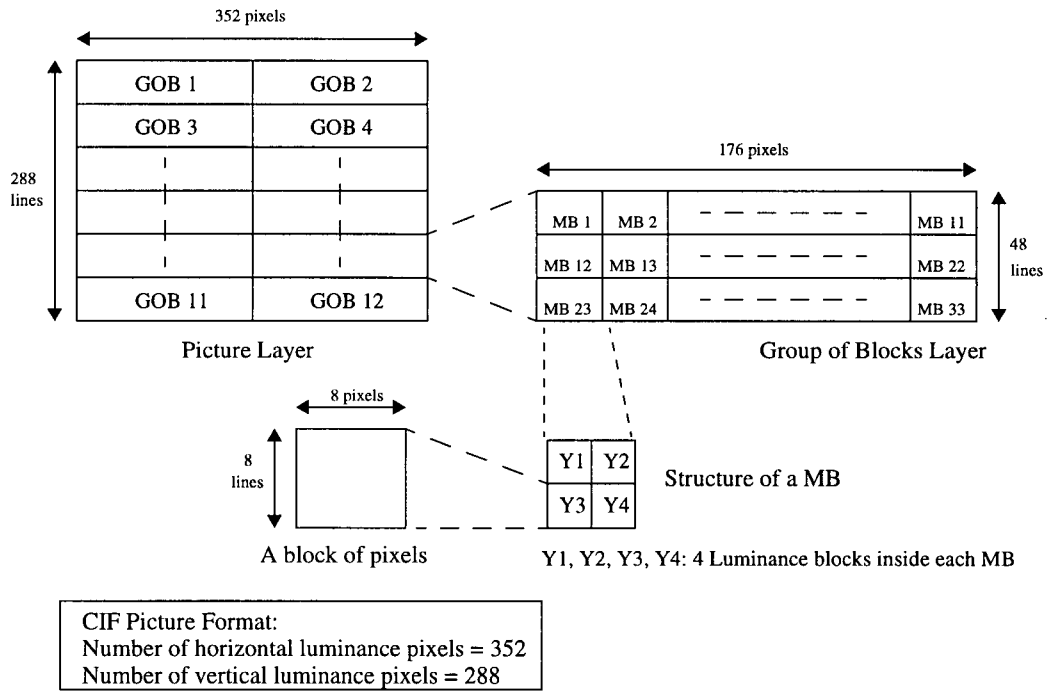

Figure 3.1. The Hierarchical Structure of the H.261 Coded Bit-stream.

In block-based motion compensation, for each MB of the current video frame being encoded, the previous video frame is searched for the corresponding best-matched MB. Then, a comparison is made between the current MB and its best-matched MB to calculate a motion

vector (MV). Using the MV, a predicted MB can be obtained by assuming that the best-matched MB from the previous video frame has been translated by the MV. The difference of pixels between the current MB being encoded and the prediction is calculated to give the prediction error. However, if there is no previous frame to obtain a prediction from, or if the best-matched MB in the previous frame is very different from the current MB such that the prediction gives large prediction error, the MB can only be intra-coded in the encoding process. The operation of the block-based motion compensation is illustrated in Figure 3.2 [19].

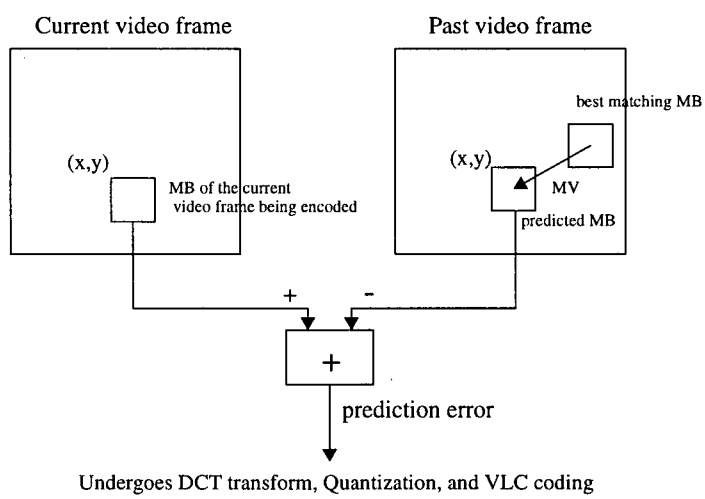

Figure 3.2. The Operation of Block-based Motion Compensation in H.261 Codec.

A transform operation of DCT is then implemented on the prediction error calculated from motion compensation. In DCT, the prediction error represented by the pixel differences is first separated into blocks of size 8x8. Each of the blocks is then transformed to give another block of 8x8 DCT coefficients. Depending on the accuracy of the prediction obtained in block-based motion compensation, the DCT coefficients can have a wide variation in characteristics. For

instance, a small prediction error will result in small pixel differences. The transformation of these small pixel differences will give small DCT coefficients. In contrast, larger DCT coefficients are produced when MB's are inaccurately predicted. The DCT coefficients are then quantized resulting in the small DCT coefficients being mapped to zero. The quantized DCT coefficients which have long runs of zeros are then variable-length (VLC) coded to achieve information compression (a detail description of the VLC coding algorithm used in H.261 can be found in [17]). Finally, the VLC-coded quantized-DCT coefficients, together with the MV's for the MB's in a video frame, can be packaged into individual video packets (the packetization scheme is explained in section 3.3.1) and sent to the decoder for image reconstruction.

3.1.2 Coded Video Bit-stream Structure

The H.261 coded video bit-stream is arranged in a hierarchical structure with four layers, as shown in Figure 3.1. These four layers, from top to bottom are: Picture layer, Group of Blocks (GOB) layer, Macroblock (MB) layer, and Block layer. The H.261 bit-stream of each video frame is composed of a picture header followed by data of GOB's, eventually followed by an end-of-sequence code (EOS) and stuffing bits. For the picture, GOB and MB layers, there are header fields which provides synchronization information for the decoder to locate the beginning and the end of these layers when it processes the coded video bit-stream.

3.2 Video Source Model

In order to evaluate the performance of the modified ATDMA access mechanism in supporting VBR video traffic, a video source model is required for the output of a VBR video codec. This section describes a modeling method which can represent the video coder output activity using a stochastic model. First, an overview of the VBR characteristics of video codec

used in videophone applications is given. Then, a stochastic model for the output of a H.261 based video codec is constructed. This model is used in this thesis to study the trade-off between the bandwidth allocation strategies of the modified ATDMA access mechanism and the quality of service (QoS) achieved by VBR video.

3.2.1 VBR Characteristics of Video Codec

In videophone applications, the VBR output characteristics of the video codec are mainly determined by the movement of an object (e.g. a face) in front of a camera. In general, the output activity of a video codec for videophone application has the following characteristics [21]:

- The video codec activity can be divided into two phases: peak phase and normal phase. The peak phase, which is the sudden increase in output bit-rate of a video codec, corresponds to scene changes such as the sudden movement of an object or the sudden change of background. The normal phase, which is the relatively constant bit-rate output of a video codec, corresponds to the relatively slight changes in the video image sequence between scene changes.
- The normal phase has a relatively longer duration than the peak phase.
- The codec activity during a given normal phase only varies slightly.
- The codec output rate in a given normal phase may be different from the rates of the neighboring normal phases. This variation in output rates depends on factors such as the extent of movement of an object during the normal phase and the complexity of the video image being encoded.

3.2.2 A Modeling Method for VBR Video Codec

In this section, a method to represent the output signal of a VBR video codec using a stochastic model is explained [22]. Experiments in [22] show that the VBR H.261 codec can be forced to transmit using a limited number of different transmission rates known as rate classes. The output activity of the resulting video coder can then be described using a discrete-time stationary Markov chain.

After encoding a video frame, the video coder in [22] will select an appropriate transmission rate class according to the size of the coded video bit-stream. The video coder will then keep transmitting at the rate chosen over the duration of one video frame. When the next video frame arrives, the video coder may then choose a new rate class depending on the size of the new video frame encoded. The video coder can achieve a piecewise constant bit rate by inserting stuffing bits to the coded video bit-stream. These additional stuffing bits can be used to transmit side information such as those for error control and for synchronization.

In [22], a typical 9 minute long head-and-shoulders video test sequence for videophone application is encoded using the H.261 codec. The video frame rate is 15 Hz and 8 permissible transmission rate classes are chosen. A "p" value of 30 has been chosen for this H.261 codec and gives a maximum bit-rate of 1.92 Mbits/s (30 x 64 kbits/s). Table 3.1 gives the statistics on the holding times and the estimated equilibrium probabilities of different transmission rate classes for the video test sequence (column 3 and 6, respectively).

Table 3.1 Statistics on Transmission Rate Classes for a H.261 Coded Video Sequence.

		Mean Holding Time (video frames)			**Equilibrium Probability**		
Rate Class No.	Transmission Rate (Mbits/s)	From statistics of video test sequence	From simulation result of the Markov chain model*	error (%)	From statistics of the video test sequence U(*j*)	From Markov chain model $\mu(j)$	error (%)
1	0.64	5.1	5.22	+2.35	0.0819	0.0842	+2.81
2	0.82	5.2	5.30	+1.92	0.2076	0.2133	+2.74
3	1.01	4.2	4.12	-1.9	0.1977	0.2015	+1.92
4	1.19	3.6	3.67	+2.05	0.1774	0.1750	-1.35
5	1.37	3.9	3.83	-1.85	0.1849	0.1797	-2.80
6	1.55	4.1	3.97	-3.13	0.1156	0.1122	-2.94
7	1.74	3.4	3.27	-3.96	0.0300	0.0292	-2.67
8	1.92	3.4	3.55	+4.51	0.0049	0.0048	-2.04

The holding time for a rate class is determined by the time span during which a video source continuously transmits at a rate specified by the rate class. The estimated equilibrium probabilities of the rate class j, U(j) (for $j = 1,\ldots, 8$), can be measured from the video test sequence as follows:

$$\mathrm{U}(j) = \frac{\text{number of video frames transmitting using rate class } j}{\text{total number of video frames in the video test sequence}} \tag{3.1}$$

In order to construct a Markov chain to describe the output of this H.261 codec, the transition probabilities between different Markov states (i.e. the different rate classes of the H.261 codec) must be obtained. The transition probability, P_{ij}, of a Markov chain is defined as the probability that a process currently in state 'i' will next be in state 'j' regardless of the process history prior to its arrival at state 'i' [23]. The transition probability, P_{ij}, from rate class 'i' to 'j' ($i,j = 1,\ldots, 8$) can be estimated using the statistics gathered from the video test sequence in [22] as

follows:

$$P_{ij} = \frac{\text{number of transitions from rate class } i \text{ to } j}{\text{number of transitions out of rate class } i} \tag{3.2}$$

The estimated transition probabilities used in the H.261 codec are shown in Table 3.2.

Table 3.2 Transition Probabilities of the Rate Classes in the H. 261 Codec {taken from [16]}.

Rate Class i	**Rate Class j**							
	1	**2**	**3**	**4**	**5**	**6**	**7**	**8**
1	0.805	0.195	0.000	0.000	0.000	0.000	0.000	0.000
2	0.077	0.808	0.115	0.000	0.000	0.000	0.000	0.000
3	0.000	0.120	0.759	0.119	0.002	0.000	0.000	0.000
4	0.000	0.002	0.132	0.721	0.144	0.001	0.000	0.000
5	0.000	0.000	0.002	0.138	0.746	0.113	0.001	0.000
6	0.000	0.000	0.000	0.004	0.179	0.754	0.063	0.000
7	0.000	0.000	0.000	0.000	0.004	0.244	0.706	0.046
8	0.000	0.000	0.000	0.000	0.000	0.000	0.282	0.718

The Markov chain model for the output of the H.261 codec can then be constructed using the transition probabilities as shown in Figure 3.3.

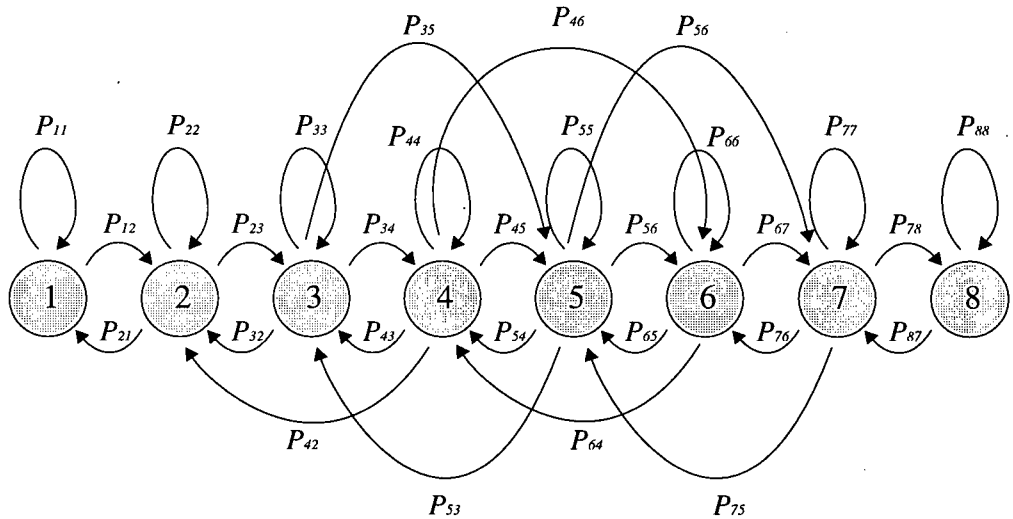

(P_{ij}, for i,j = 1,2,..., 8 is the transition probability from state i to j)

Figure 3.3. A Markov Chain Model of the H.261 Video Codec.

Using the transition probabilities in Table 3.2 and the Markov chain model in Figure 3.3, the equilibrium probabilities for the 8 transmission rate classes of the Markov chian, $\mu(j)$ (for j = 1,...., 8), can be calculated by solving the following equations:

$$\mu(j) = \sum_{i=1}^{8} \mu(i) P_{ij}, \qquad i,j = 1, 2, \ldots, 8 \tag{3.3}$$

$$\sum_{j=1}^{8} \mu(j) = 1 \tag{3.4}$$

In Table 3.1, a comparison has been made between the computed equilibrium probabilities of the Markov chain ($\mu(j)$) and the corresponding measured values obtained from the video test sequence U(j). A simulation model has also been built for the Markov chain in Figure 3.3 using

Ptolemy [13]. This simulation model has been set to run for a simulation time of 9 minutes (same duration as for the video test sequence) and the mean holding times of different rate classes are measured and listed in column 4 of Table 3.1. The agreement between the statistics measured from the video test sequence and those obtained from the Markov chain model shows that the method proposed in [22] can model the output of the H.261 codec. A sample output of the Markov chain model for the H.261 codec (which represents the output for a duration of 300 video frames) has been generated using Ptolemy and is shown in Figure 3.4.

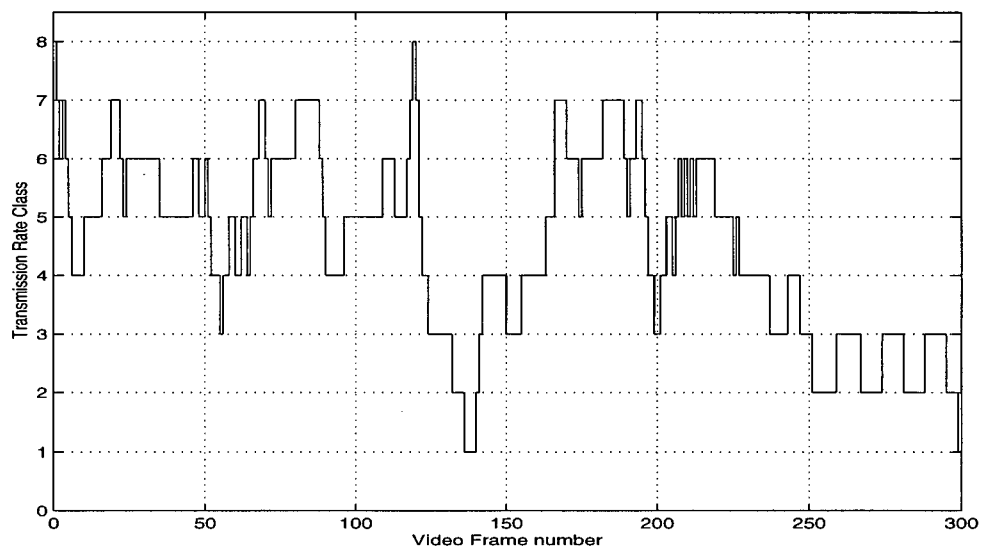

Figure 3.4. A Sample Output of the Markov Chain Model for the H.261 Video Codec.

3.2.3 Stochastic Model for a Modified H.261-based Video Codec

Recent advances in source coding technology has made possible the development of more advanced H.261-based video codecs which produce lower bit-rate outputs when compared to the original H.261 codec. In 1995, the ITU-T developed the H.263 codec; this codec, having a maximum bit rate of 28.8 kbits/s for videophone application, is an example of a modified H.261-

based video codec. The design of the H.263 codec is based on the H.261 standard, in particular, in the concepts of macroblocks, motion compensation, and transform coding [24]. The lower bit rate of the H.263 codec is achieved using a more efficient coding method for motion vectors, DCT coefficients and other overhead information of video signal [25].

The modified H.261-based video codec which generates a lower bit-rate output is more suitable for supporting audio-visual applications in the bandwidth limited wireless environment. In order to construct a Markov chain model for the modified H.261-based video codec using the method described in section 3.2.2, statistics on the VBR characteristics of the output bit-stream are required. Since the modified and the original H.261 codecs use the same mechanism to encode motion pictures, their output bit-streams are assumed to have similar VBR characteristics. As a result, this thesis uses the VBR characteristics of the original H.261 codec as a reference for the construction of the Markov chain model for the modified H.261-based codec.

In this thesis, it is assumed that, through the application of a more efficient coding method for motion vectors, DCT coefficients and other overhead information of video signal, the maximum bit-rate of the modified H.261-based codec can be lowered to 28.8 kbits/s (same as the bit-rate of the H.263 codec). Therefore, the ratio of the maximum transmission rate of the modified codec to that of the H.261 codec used in [22] (where a "p" value of 30 is chosen) is 0.015 (i.e.(28.8 kbits/s)/ (1.92 Mbits/s) = 0.015). By applying this scaling factor to the allowable transmission rate classes for the H.261 codec used in [22] (column 2 of Table 3.3), the respective transmission rates that would be required by the modified H.261-based codec can be estimated and are shown in column 3 of Table 3.3.

Table 3.3 Estimated Transmission Rates of the H.261-based Video Codec.

H.261 codec rate class no.	H.261 transmission rate (Mbits/s)	Estimated equivalent transmission rate for the modified H.261-based codec (kbits/s)	Gross bit rate of modified H.261-based codec after channel coding (kbits/s)	Number of time-slots per transmission frame required by the modified H.261-based codec	Rate class no. for the modified H.261-based codec
1	0.64	9.60	15.63	2	1
2	0.82	12.30	20.03	2	1
3	1.01	15.15	24.67	2	1
4	1.19	17.85	29.06	3	2
5	1.37	20.55	33.46	3	2
6	1.55	23.25	37.86	3	2
7	1.74	26.10	42.50	4	3
8	1.92	28.80	46.89	4	3

In a wireless environment, a powerful forward error correction (FEC) code is necessary to protect the low bit-rate video bit-stream so that it can be successfully transmitted at acceptable power levels. In this thesis, a BCH(127, 78, 7) code is assumed which has shown to provide sufficient error protection to the H.263 coded video in a wireless environment [15]. The BCH(127, 78, 7) code which has a code rate of (78/127) will add additional overhead bits to the modified H.261-based coded video after channel coding. Column 4 shows the gross bit rates for the respective transmission rates in column 3 after channel coding. Since one time-slot per transmission frame in the ATDMA system can support a connection rate of 13.2 kbits/sec, column 5 displays the respective number of time-slots per transmission frame that are required to support the gross bit-rates listed in column 4. By grouping the gross bit-rates which require the same number of time-slots per transmission frame, three transmission rate classes (class 1, class2, and class 3) can be assigned to the modified H.261-based video codec. Class 1 corresponds to a transmission rate of 26.4 kbits/s which requires two time-slots per transmission frame. The

transmission rates for class 2 and 3 require three time-slots (39.6 kbits/s) and four time-slots per transmission frame (52.8 kbits/s), respectively.

Let $\mu'(n)$, $n = 1,2,3$, and P'_{mn}, $m,n = 1,2,3$, be the equilibrium probabilities and the transition probabilities for the three rate classes of the modified H.261-based codec, respectively. $\mu'(n)$, $n = 1,2,3$, and P'_{mn}, $m,n = 1,2,3$, can be estimated using the equilibrium probabilities $\mu(j)$, $j = 1,2,...8$, and transition probabilities P_{ij}, $i,j = 1,2,...8$, of the original H.261 codec, respectively. The calculation for $\mu'(n)$ is as follows:

$$\begin{aligned} \mu'(1) &= \mu(1) + \mu(2) + \mu(3) = 0.499 \\ \mu'(2) &= \mu(4) + \mu(5) + \mu(6) = 0.467 \\ \mu'(3) &= \mu(7) + \mu(8) = 0.034 \end{aligned} \tag{3.5}$$

The transition probability P'_{mn} of the modified H.261-based codec can then be calculated using $\mu'(n)$ and the information provided in Table 3.3. The calculation of P'_{21} is shown as an example to illustrate the procedure. For the modified H.261-based codec, the probability of having a rate class transition from class 2 to class 1, i.e Pr{class 2 to 1}, can be calculated using Equation 3.6.

$$\Pr\{\text{class 2 to 1}\} = \mu'(2) \times P'_{21} \tag{3.6}$$

According to the relationship between the rate classes of the modified H.261-based codec and the H.261 codec shown in Table 3.3, Pr{class 2 to 1} can also be calculated as shown in Equation 3.7.

$$\Pr\{\text{class 2 to 1}\} = \mu(4) \cdot [P_{43} + P_{42}] + \mu(5) \cdot P_{53} \tag{3.7}$$

By equating Equations (3.6) and (3.7), and dividing both sides by $\mu'(2)$, the proabability P'_{21} can be calculated as follows:

$$P'_{21} = \frac{\mu(4)[P_{43} + P_{42}] + \mu(5)P_{53}}{\mu'(2)} \tag{3.8}$$

Similarly, the probability P'_{23} can be obtained as shown in Equation (3.9).

$$P'_{23} = \frac{\mu(6)P_{67} + \mu(5)P_{53}}{\mu'(2)} \tag{3.9}$$

Finally, Equation 3.10 can be used to calculated P'_{22}.

$$P'_{22} = 1 - P'_{21} - P'_{23} \tag{3.10}$$

By using the same procedure, the probability P'_{1n} and P'_{3n}, n = 1,2,3, can be calculated as in Equations (3.11) and (3.12).

$$\begin{aligned} P'_{12} &= \frac{\mu(3)[P_{34} + P_{35}]}{\mu'(1)} \\ P'_{13} &= 0 \\ P'_{11} &= 1 - P'_{12} - P'_{13} \end{aligned} \tag{3.11}$$

$$\begin{aligned} P'_{32} &= \frac{\mu(7)[P_{76} + P_{75}]}{\mu'(3)} \\ P'_{31} &= 0 \\ P'_{33} &= 1 - P'_{32} - P'_{31} \end{aligned} \tag{3.12}$$

The resulting matrix of transition probabilities for the three rate classes of the modified H.261-based codec is shown in Table 3.4.

Table 3.4 Transition Probabilities of the Modified H.261-based Codec.

Rate Class m	Rate Class n		
	1	2	3
1	0.951	0.049	0.000
2	0.051	0.934	0.015
3	0.000	0.213	0.787

Based on Table 3.4, a Markov chain model can be constructed as shown in Figure 3.5. This Markov chain is stationary and it has a simple structure where transitions only occur to the neighboring transmission rate classes.

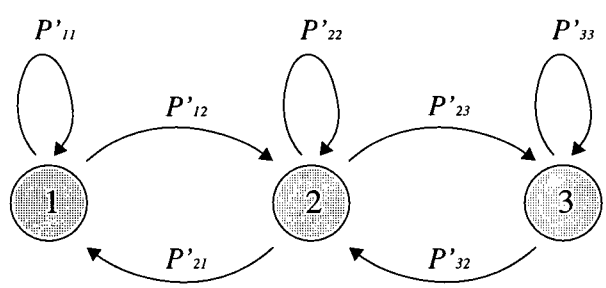

P'ij, (for i,j = 1,2,3), is the transition probability from Markov state i to j

Figure 3.5. A Markov Chain Model of the Modified H.261-based Codec.

The modified H.261-based video source model used in this thesis, therefore, has three permissible transmission rate classes. At the start of a video frame, the modified H.261-based video coder will select an appropriate rate class depending on the size of the coded bit-stream. The video coder maintains the same transmission rate specified by the rate class over a time period of one video frame. When a new video frame arrives, a new transmission rate class may be

chosen according to Figure 3.5, if necessary. The result is a piecewise constant bit-rate video source which can be described by the Markov model in Figure 3.5.

Figure 3.6 illustrates a sample output of the Markov chain model of the modified H.261-based codec. This sample is obtained from a computer simulation of the Markov chain model which lasts for 500 video frames.

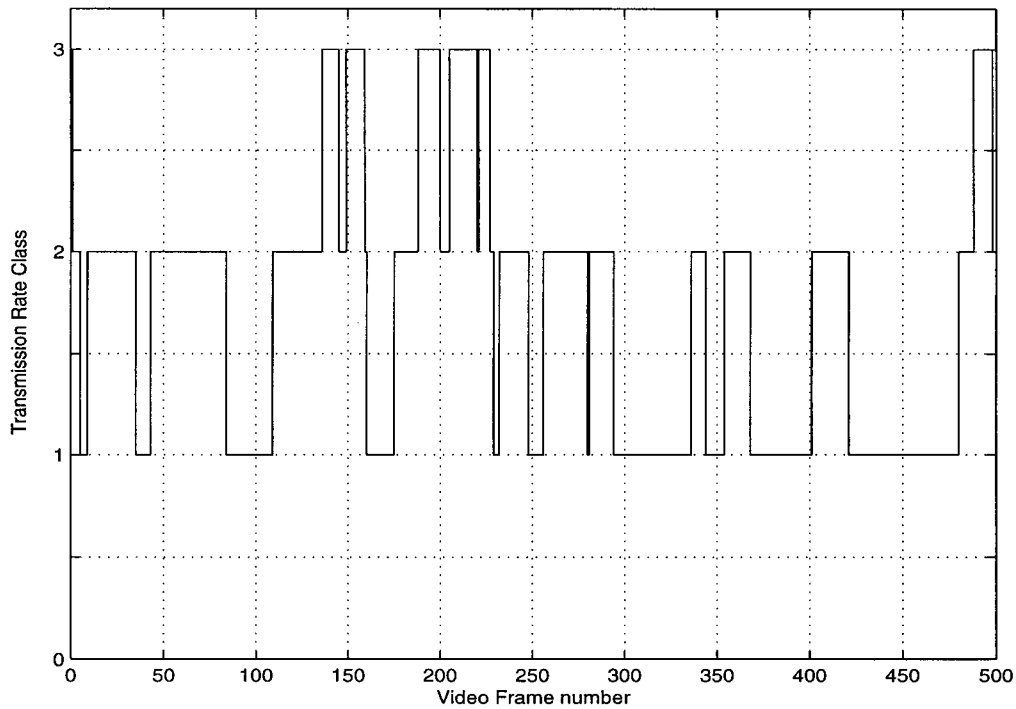

Figure 3.6. A Sample Output of the Markov Chain Model of the Modified H.261-based Codec.

3.3 Packetization Scheme for Modified H.261-based Codec

In this section, a packetization scheme which converts the modified H.261-based coded bit-stream into individual packets suitable for transmission in the ATDMA system is introduced. As described in Chapter 2, the PRMA++ access mechanism of the ATDMA system operates in a

Time Division Multiple Access (TDMA) structure in which a transmission frame (5 ms duration) is divided into 72 equal size time-slots. Mobiles transmit their information streams by sending information bursts (as shown in Figure 2.2) in the information slots (I-slots) of the transmission frame. Since the size of each I-slot is fixed to carry 66 information bits, video coders need to packetize their coded bit-streams such that a video packet can be accommodated in the I-slot of the ATDMA system.

Figure 3.7 shows the structure of a video packet. Each video packet has a size of 66 bits, and thus, can be carried by one I-slot of the ATDMA system.

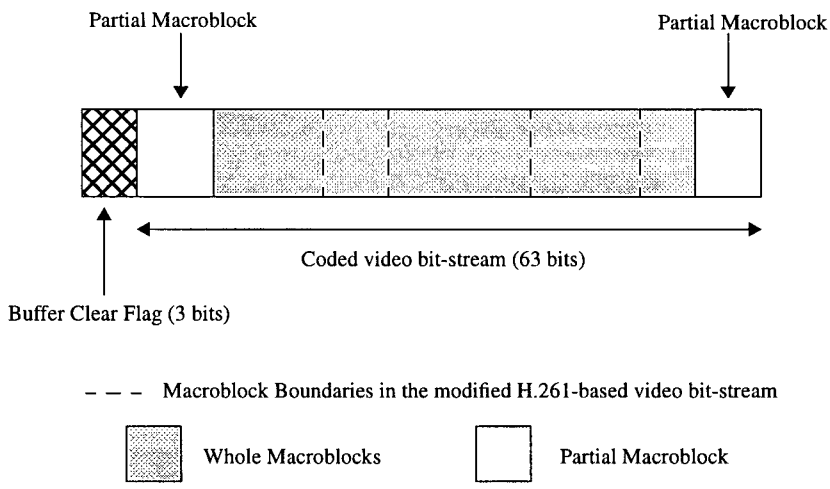

Figure 3.7. Structure of a Packet Generated by the Modified H.261-based Video Codec.

In Figure 3.7, a video packet is divided into a data area (63 bits) and a buffer-clear flag of 3 bits. The data area contains the coded marcoblocks of a video frame. The sizes of the macroblocks are different (as shown in Figure 3.7) due to the different results obtained from the block-based motion compensation of the macroblocks as illustrated in section 3.1.1. Therefore, the number of

macroblocks that each video packet can carry is a variable. Marcoblocks that cannot be accommodated completely in one video packet may need to be carried as partial macroblocks in two video packets.

The header information of each macroblock informs the receiver the position of the last whole macroblock fully contained within a video packet (as described in Section 3.1.2). When a video packet is received at the receiver, the partial macroblock is buffered until the remainder carried by another video packet arrives. However, if the video packet which carries the remainder of a buffered partial macroblock is lost due to packet dropping (video packet dropping is explained in the section 3.5), the video coder will set the buffer-clear flag in the following video packet transmitted to inform the receiver to discard the buffered partial macroblocks. By buffering the partial macroblock temporarily, the receiver only passes whole macroblocks to the video decoder for decoding, thus, ensuring that there are no errors in the output video caused by partial macroblocks. When a video packet is dropped, the receiver will replace the macroblocks and the partial macroblock that the dropped packet contains by a codeword to inform the decoder to process these macroblocks as unchanged from the previous video frame.

In order for the receiver to update the information contained in the macroblocks that have been lost, a modification of the video coding algorithm is required [26]. The H.261-based coder needs to record those unsuccessfully transmitted macroblocks due to packet dropping. When video coding proceeds in the next video frame, the video coder will specially encode those macroblocks affected by packet dropping so that the lost information can be updated at the receiver in the next video frame. This can be achieved by keeping a history of various parameters for each macroblock at the video coder. By using the parameters, the video coder can reconstruct

the best-matched macroblocks of the those macroblocks that have been lost due to packet dropping. When the encoding process proceeds in the next video frame, the reconstructed best-matched macroblocks will be used in the process of motion-compensation for those macroblocks affected by the packet dropping. Therefore, the information loss caused by packet dropping can be updated in the next video frame and stop the decoding error propagating in the temporal domain of a video sequence. When a video packet is successfully transmitted to the receiver, the video coder will discard the parameters associated with the macroblocks contained within the packet.

3.4 Modified ATDMA Access Mechanism

In this section, a modified ATDMA access mechanism is proposed. The ATDMA access mechanism in [5] is designed primarily for supporting voice and data services in which the base station assigns a fixed number of time-slots (i.e. a fixed bandwidth) to a connection during its period of activity. However, the assignment of a fixed bandwidth to a connection which exhibits VBR characteristics (e.g. video) might lead to a wastage of bandwidth during its period of low activity. The proposed modifications of the access mechanism will enable the base station of the ATDMA system to assign a varying number of time-slots (i.e. a varying amount of bandwidth) to the modified H.261-based video connection (which exhibits VBR characteristics) on a demand basis.

3.4.1 Establishment of a Video Connection

A video connection establishment procedure consists of the following two phases:

- *Mobile ID Assignment Phase:* Each video terminal has its own subscriber ID. When a video terminal is switched on, it will request a mobile ID (for usage in the cell) by transmitting its subscriber ID in a call set-up initialization (CSI) burst (Figure 2.3) in the next available reservation slot (R-slot) on the up-link. The base station will then check the subscriber ID for the authentication of the video terminal. If the terminal can be accepted into the cell, the base station will send a mobile ID to the video terminal in the paired acknowledgment slot (A-slot) on the down-link.

- *Call Set-up Phase:* When a video connection needs to be established, the video terminal transmits a reservation burst (Figure 2.4) in the R-slot to request an I slot in which to send a call set-up message. After receiving an I slot assignment through the A-slot on the down-link, the video terminal then sends a set-up message which contains the subscriber ID of the terminal being called and other information such as the QoS required by the connection. After that, the video terminal will listen to the A slot on the downlink until a reply (an ack-set-up message) is received from the base station. The ack-set-up message indicates either a "busy" or "idle" signal to the video terminal. The "busy" signal indicates that the called terminal is currently busy or no network resources are available to support the connection at this time. After receiving a "busy" signal, the video terminal needs to "hang-up" and re-send the set-up message at a later time. On the other hand, an "idle" signal indicates that the called terminal has been connected and the network resources are available for the requested connection.

Figure 3.8 is a time sequence diagram to illustrate the connection establishment procedure. After completion of the connection establishment procedure, the video terminal enters the information transfer phase which is described in the next sub-section.

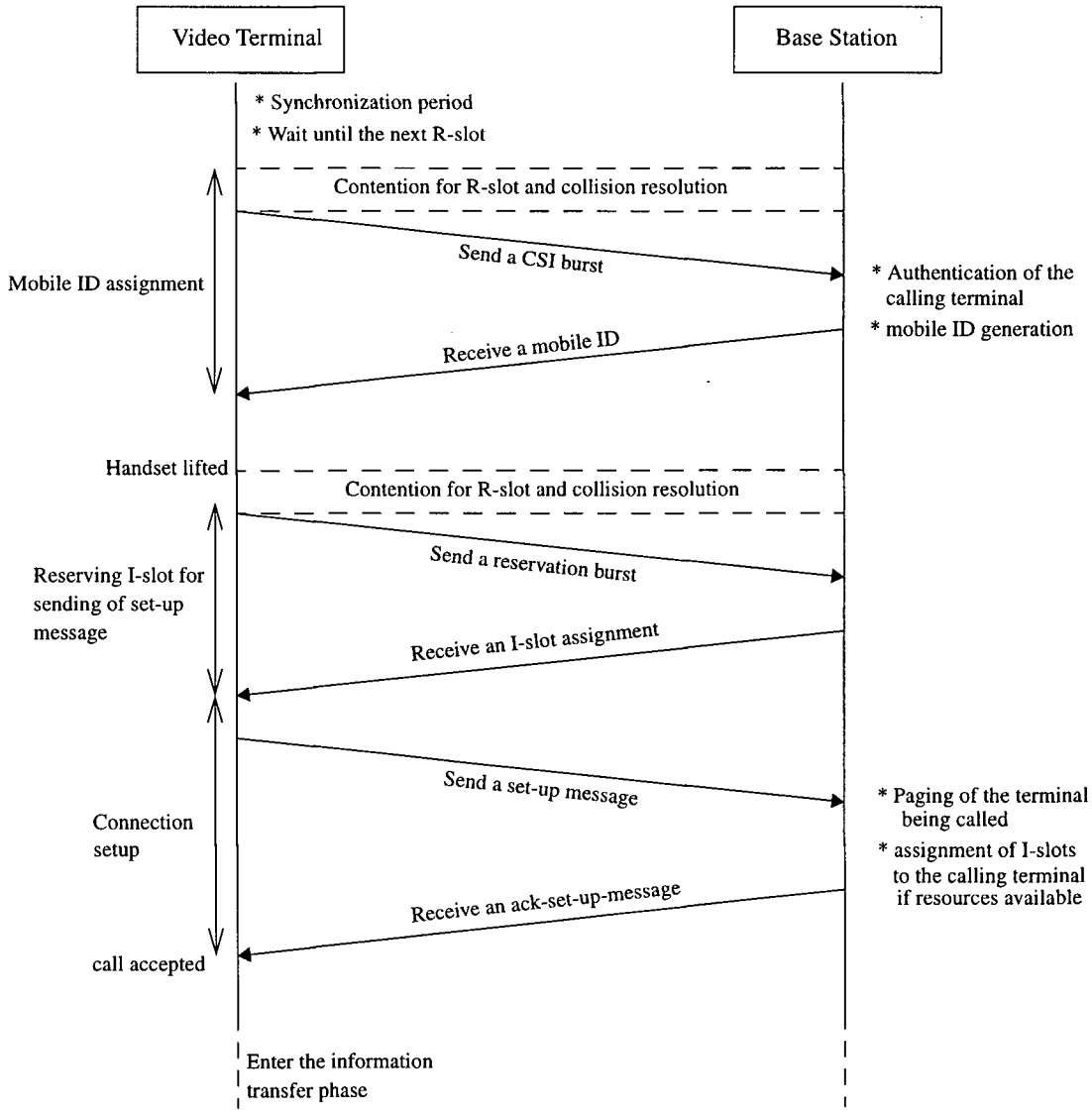

Figure 3.8. Information Flow Between a Video Terminal and the Base Station During the Mobile ID Assignment and the Call Set-up Phases.

3.4.2 Information Transfer Phase for Video Connection

After a video connection has been established, the video terminal will start scanning and encoding a video frame every 66.7 ms (assuming a video frame rate of 15 Hz). The first frame of a video sequence can only be intra-coded since no previous video frame is available for the implementation of inter-frame coding to reduce the temporal redundancy. This intra-coded video frame results in a larger size of the coded bit-stream than that of the following video frames which can use block-based motion compensation in video compression. As a result, the base station needs to assign 4 I-slots per transmission frame (class 3, the highest transmission rate class) to the video connection at the moment it is accepted into the system. The assignment of these 4 I-slots can be included in the ack-set-up message when a connection has been established for the video terminal. After receiving the I-slots assignment, the video coder will then maintain the 'class 3' transmission rate by using the same four I-slots in the following transmission frames for transmitting the video packets of the first video frame.

When the video coder encodes the next video frame, the size of the coded bit-stream of the new video frame may be different from the previous one. As a result, one of the following three situations may occur at the arrival of a new video frame:

- *Maintenance of the same transmission rate class:* In this case, the video terminal determines that the coded bit-stream of the new video frame can be transmitted to the receiver by keeping the same transmission rate as for the previous video frame. The video coder will just continue to transmit the video packets of the new video frame in the same sequence of I-slots that it has reserved in the previous video frame. No further reservation request needs to be sent from the video terminal to the base station.

The base station, in this case, will assume that the video terminal continues to reserve the same I-slots sequence in the following transmission frames for transmitting the video packets of the new video frame.

- *Transition to a lower transmission rate class:* According to the video source Markov chain model in Figure 3.5, transitions only occur to neighboring states. Therefore, a switch to a lower transmission rate class means that one of the I-slots used by the video terminal in the previous video frame is not used in the new video frame. The surplus I-slot, therefore, needs to be released back to the base station so that it can be allocated to another user in the next transmission frame. The releasing of the extra I-slot can be achieved through the in-band signalling feature provided in the I-slots. By sending a signalling message in the surplus I-slot, the video terminal can inform the base station that the I-slot can be retrieved and re-allocated to another user in the next transmission frame. The base station assumes that the video terminal continues to reserve the remaining I-slots for transmitting the video packets of the new video frame.

- *Transition to a higher transmission rate class:* According to Figure 3.5, a transition to a higher transmission rate class means that an extra I-slot must be assigned to the video terminal in the new video frame. Similarly, the video terminal can request the base station for an extra I-slot through in-band signalling. As soon as a video terminal finished encoding a new video frame and decides to switch to a higher transmission rate class in the new video frame, it will send a signalling message in the next available I-slot of the I-slot sequence reserved since the previous video frame. After sending the signalling message, the video terminal will listen to the next available acknowledgment slot (A-slot) on the down-link to receive an answer of the request. For video ser-

vice, the base station will allocate the free I-slots to the video terminals requesting for higher transmission rate classes on a "first come first serve basis". Video terminals which do not receive allocation in the A-slot will wait and keep monitoring the following A-slots of the transmission frames. Besides using the extra I-slot assigned in the new video frame, the video terminal also maintain the reservation of the I-slot sequence reserved since the previous video frame for transmitting the video packets of the new video frame.

3.5 Video Packet Access Delay Threshold and Dropping

In real-time audio-visual applications such as videophone and video-conferencing, the coded bit-streams of video sequences are delay sensitive and require prompt delivery. Furthermore, the "lip synchronization", which refers to the temporal relationship between the audio and video signals in human speaking, must be maintained [27].

At the arrival of a new video frame, the video terminal requesting for higher transmission rate classes must listen to the base station for the extra I-slot assignment. Depending on the traffic load of the system, the video terminal may need to wait in the I-slot allocation queue if no I-slot is currently available. A delay in accessing an extra I-slot will increase the total time required to transmit all the video packets of a video frame. In voice service, an access delay of 10 ms is acceptable for voice packets. Since this thesis intends to investigate the efficiency of the ATDMA system in supporting low resolution video which can be used in audio-visual applications, the 10ms access delay threshold is also applied to the video packets in accessing channels (i.e. I-slots). The 10 ms access delay threshold for video packets means that the maximum allowable

delay for transmission of a video packet is 10 ms after the end of the video frame. The video packets of a video frame which cannot be transmitted before this deadline will be dropped. The decoder will process those macroblocks which are lost due to packet dropping as "unchanged" from the previous video frame. The video coder can use the information updating scheme described in section 3.3 to enable the receiver to update the information contained in the macroblocks which are dropped.

Experiments on human perception has been performed to investigate the effects of video packet dropping on video degradation. In [26], studies show that a 3% video packet loss rate is considered to be acceptable by observers (for H.263 codec operating at a video frame rate of 15 Hz).

Chapter 4 Performance Evaluation of Video Service Using the Modified ATDMA Access Mechanism

This chapter uses computer-simulation to evaluate the performance of the modified ATDMA access mechanism in supporting low resolution video which exhibits VBR characteristics. A discrete event simulator, Ptolemy [27], is used in this thesis to model and implement the modified ATDMA access mechanism. This chapter is divided into four sections. The first section lists the working assumptions used in the simulation. The second and third section study the access delay and the video packet dropping probability of video services, respectively. The last section gives a performance measure of the proposed access mechanism based on the simulation results.

4.1 Assumptions

The working assumptions used in the computer simulation are as follows:

1. System Parameters:
   - *TDMA frame structure*: The same TDMA frame structure as described in Table 2.1 of Chapter 2.
   - *Channel error*: Error-free channel, such that failed transmission results only from video-packet dropping due to excessive channel access delay.
   - *Acknowledgment delay*: An acknowledgment delay of 3 time-slots (i.e. 208 μs) is assumed. Therefore, after sending a request for an additional I-slot through in-band signalling, a video source starts listening to the closest A-slot on the down-link which is at least 3 time-slots away.

2. Video source parameters:
    - *Video source model*: A video source model with three permissible transmission rate classes as described in Section 3.2.3 of Chapter 3 is used. The video frame rate is 15 frames/ second.
    - *Video packet size*: 66 bits (the packetization scheme is described in Section 3.3 of Chapter 3).
3. QoS assumptions for video source:
    - *Access Delay:* Access delay is defined as the time which elapses from the moment that a video source switches to a higher transmission rate class to the instant that transmission starts in an additional I-slot assigned by the base station. An access delay threshold of 10 ms is applied to video service. Therefore, video packets which cannot be transmitted within 10 ms after the end of a video frame will be dropped. Furthermore, a 5-percentile access delay threshold of 76.7 ms is also assumed (one video frame duration of 66.7 ms plus an access delay threshold of 10 ms). The 5-percentile access delay threshold ensures that 95% of the I slot requests can have I-slots allocated within 76.7 ms such that no video packet loss (caused by excessive access delay) will occur in the second video frame after a video source has switched to a higher transmission rate class. Therefore, lost information of a video frame due to packet dropping can be updated in the subsequent video frame using the information up-dating scheme as described in section 3.3 of Chapter 3.

- *Packet loss*: As video sources switch to higher transmission rate classes, video packets may be lost due to excessive access delay. A 3% video packet loss of the first video frame after rate class increase is assumed as the packet loss threshold for video service.

4. Length of channel time simulated:
   - *Warm-up time*: 100 seconds.
   - *Statistics gathering time*: 1000 second.

4.2 Access Delay of Video Service using the Modified ATDMA Access Mechanism

In the modified ATDMA access mechanism, the overall access delay experienced by video service has three components, which are illustrated in Figure 4.1.

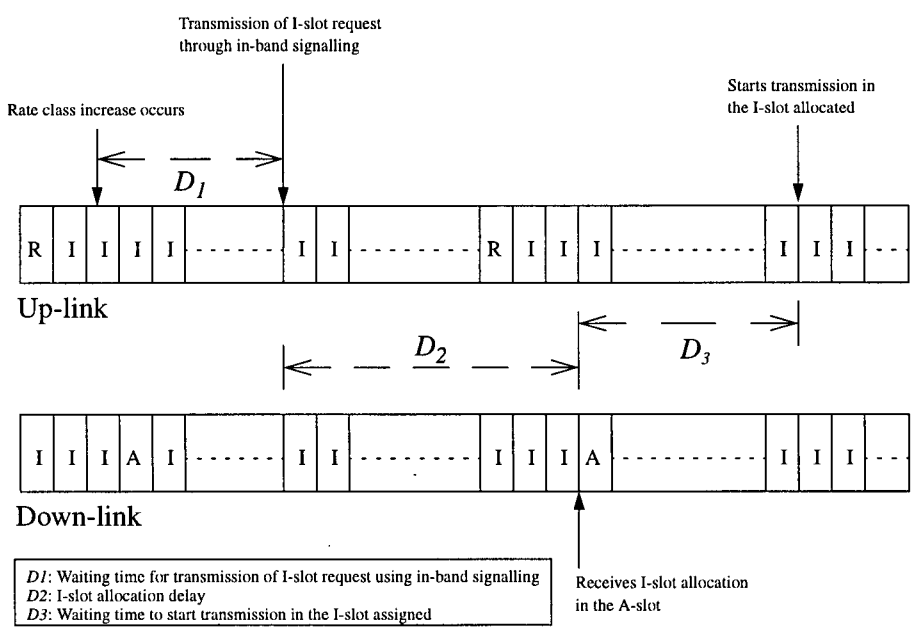

Figure 4.1. The Three Components (D_1, D_2, D_3) of the Access Delay.

The three components of the access delay are described as follows:

- *Waiting time for transmission of I-slot request using in-band signalling (D1)*: when a video source switches to a higher transmission rate class, it needs to inform the base station through in-band signalling in the first available I-slot of the I-slot sequence (i.e. the I-slots that a video terminal has reserved since the previous video frame). Thus, there is a waiting time which has elapsed from the moment of rate class increase to the instant that a reservation request can be sent in the first available I-slot. Depending on the timing of the rate class increase and on the position of the first available I-slot that a video source can use to send an I-slot request, *D1* has a value which ranges from a minimum of 0 ms (the best case) to a maximum of 4.861 ms (the worst case). For instance, the best case occurs if a rate class transition happens at the beginning of an I-slot that the video source has already reserved; therefore, the video source can use the I-slot immediately to request for an extra I-slot through in-band signalling. In contrast, the worst case occurs, for example, when a rate class transition occurs at time *a* (refer to Figure 4.2) and the video source has reserved slot # 71 and 72 since the previous video frame (because the lowest transmission rate class, i.e. class 1, of a video connection requires two I-slots per transmission frame; therefore, the video source must have at least reserved two I-slots per transmission frame since the previous video frame). This worst situation will give a maximum *D1* of 4.861 ms (i.e. 70 slots x 0.06944 ms/slot = 4.861 ms).

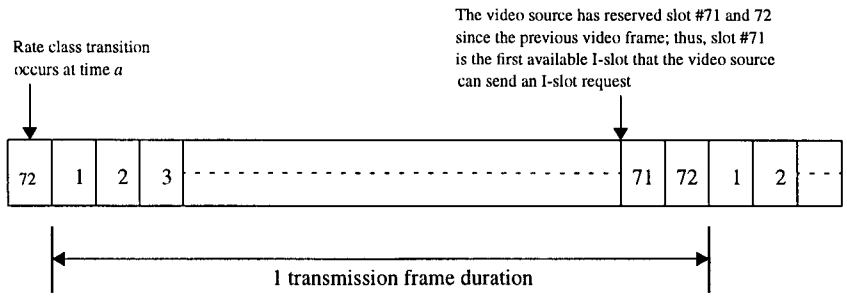

Figure 4.2. Illustrating a Maximum *D1* Value of 4.861 ms.

- *I-slot allocation delay (D2):* After sending a reservation request through in-band signalling, a video source must listen to the next available acknowledgment slot (A-slot) on the down-link (which is at least 3 time-slots away) for I-slot assignment. If no assignment is made to the video terminal, the video terminal needs to wait and keep monitoring the following A-slots on the downlink until an assignment is received. The time that has elapsed from the transmission of reservation request to the reception of I-slot assignment is called the I-slot allocation delay *(D2)*. *D2* depends on two factors. First is the response time of the base station, which is defined as the shortest time interval between two consecutive I-slot assignments that can be made by the base station. The second factor is the availability of free I-slots that can be assigned to video sources requesting for higher transmission rate classes. The first factor depends on the number of A-slots per transmission frame on the down-link, while the second factor depends on the traffic load being supported in the ATDMA system. A further description of these two factors will be given later in this section.

- *Waiting time to start transmission in the I-slot assigned (D3):* When a video terminal receives an I-slot assignment in the A-slot on the downlink, there is a delay before transmission starts in the extra I-slot allocated (*D3*). Since the base station uses a random slot-allocation policy as described in Section 2.3.3 of Chapter 2, depending on the location of the extra I-slot assigned, the length of *D3* ranges from a minimum of 69.4 μs (1 time-slot duration) to a maximum of 5ms (72 time-slot duration).

Among the three components of the overall access delay, *D1* and *D3* are both confined within a fixed range (0 ms to 4.861 ms for *D1*, 69.4 μs to 5ms for *D2*). However, *D2* has no fixed range of value and its magnitude depends both on the response-time of the base station and on the traffic-load being supported by the ATDMA system. In order to control the access delay experienced by video sources in the ATDMA system (which in turn affects the video packet dropping probability), the factors which affect *D2* must be studied.

Since the I-slot allocation delay (*D2*) depends on the response time of the base station, *D2* can be reduced by using more R-slots per transmission frame. As the number of R-slots per transmission frame increases, the number of A-slots on the down-link increases accordingly due to the pairing nature of the R and A-slots used in the ATDMA system. The increased number of A-slots per transmission frame can reduce the time interval between two consecutive I-slot assignments that can be made by the base station (i.e. the response time is reduced). Therefore, using more R slots per transmission frame may result in a decrease in the access delay of video sources by reducing their waiting time to receive assignments from the base station. This advantage is more obvious under low traffic-load conditions in which free I-slots are always available for allocation to reservation requests. As a result, the only determinant of the I-slot allocation delay (*D2*) under the low traffic-load condition becomes the response time of the base

station.

Figure 4.3 depicts an example scenario which can illustrate how the usage of more R-slots per transmission frame can reduce the I-slot allocation delay under low traffic-load conditions. In Figure 4.3, the part of a transmission frame on the up-link which is confined between two consecutive R-slots is known as a transmission sub-frame. The size of a sub-frame, n, is determined by the number of time-slots that it contains. In sub-frame #1, two video sources (source #1 and #2) send I-slot requests to the base station in slot I_a and I_b, respectively. After transmission of I-slot requests, the mobiles will wait in the I-slot allocation queue and they will be served by the base station on a first-come first-serve basis. The I-slot allocation delay ($D2$) can be divided into two components. First, is the waiting time, W_i (as shown in Figure 4.3), of a video source #i which measures the number of time-slots that elapses from the moment of I-slot request transmission to the arrival of the first A-slot on the down-link which is at least three time-slots away. The second component is the queueing delay, defined as the duration that a video source needs to wait in the I-slot allocation queue. Assuming that there are j video sources waiting in I-slot allocation queue at the beginning of the transmission sub-frame #1 and that free I-slots are always available under the low traffic-load condition, $D2_1$ and $D2_2$ are the I-slot allocation delay for source #1 and #2, respectively.

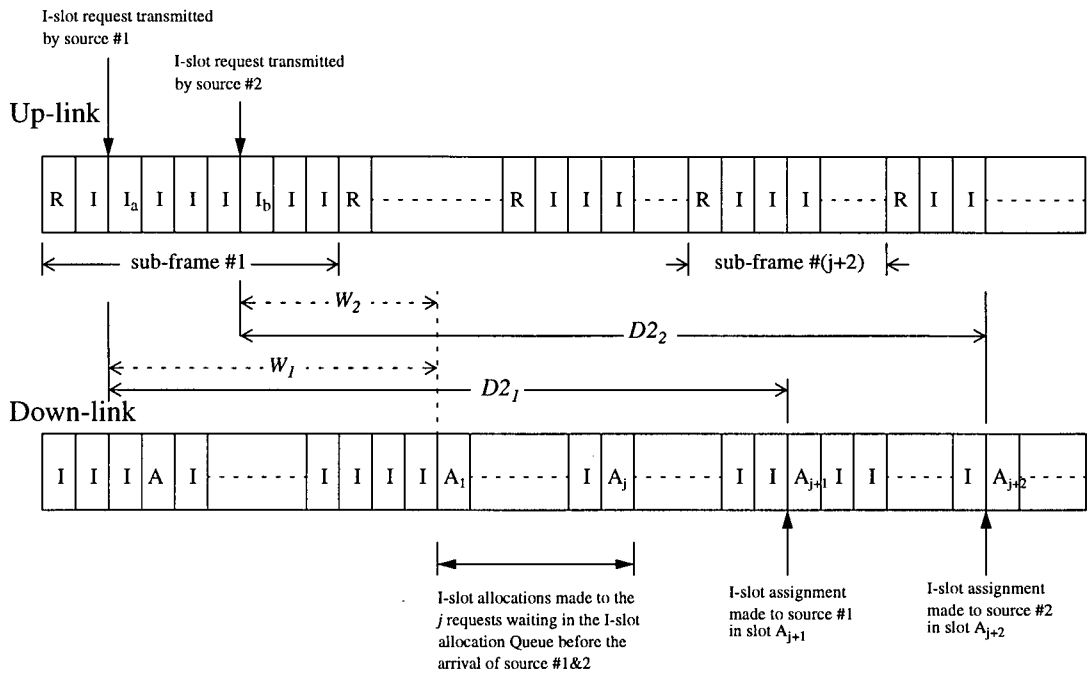

Figure 4.3. An Example Scenario which Illustrates the Components of I-slot Allocation Delay (*D2*).

It is observed that the delay, $D2_i$, of a video source *#i* under the low traffic-load condition is determined by the waiting time, W_i, and on the size of the I-slot allocation queue at the moment that an I-slot request is transmitted. Assuming that t is the duration of 1 time-slot (i.e. 0.0694 ms) and j is the size of the I-slot allocation queue at the moment of I-slot requests transmission, the I-slot allocation delay for video source *#i* ($D2_i$) under low traffic-load condition can be estimated as follows:

$$D2_i = \{W_i + n \cdot j\} \cdot t \tag{4.1}$$

Equation 4.1 shows that $D2_i$ depends on n, W_i and j. By reducing the size of the transmission sub-frame, n, through the use of more R slots per transmission frame, the following effects

on the waiting time, W_i, and on the size of the I-slot allocation queue, j, are expected.

- The mean waiting time, $\overline{W_i}$, of video source i decreases as n decreases. Since the base station uses a random slot-allocation policy, each I-slot within a transmission sub-frame has the same probability to be used for transmission of I-slot request by video sources through in-band signalling. Taking into account the three time-slots temporal offset between each paired R and A slots (as illustrated in Figure 4.2), $\overline{W_i}$ for video source #i can be estimated using Equation 4.2. It is observed that $\overline{W_i}$ is proportional to the size of the transmission sub-frame (i.e. n); therefore, a reduction in n leads to a reduction in $\overline{W_i}$.

$$\begin{aligned}\overline{W_i} &= \left\{\left(\frac{1}{(n-1)} \cdot \sum_{i=1}^{(n-1)} i\right) + 3\right\} \text{ slots} \\ &= \frac{(n+6)}{2} \text{ slots}\end{aligned} \tag{4.2}$$

- When free I-slots are always available, the base station of the ATDMA system can make one I-slot allocation in the A-slot following each transmission sub-frame. Therefore, video sources under the low traffic-load condition starts queueing up in the I-slot allocation queue only when more than one I-slot requests are received through in-band signalling within a transmission sub-frame. As n decreases, the number of I-slots within a transmission sub-frame decreases accordingly. Therefore, the probability of receiving multiple I-slot requests within a transmission sub-frame will decrease which causes fewer number of video sources to queue up in the I-slot allocation queue (i.e j will decrease).

Therefore, using more R-slots per transmission frame can reduce the I-slot allocation delay (*D2*) of video sources under low-traffic-load condition, and may eventually lead to a lower overall access delay. Figure 4.4 shows the mean access delay of video sources, when there are 9 to 20 video connections established in the ATDMA systems using different number of R-slots per transmission frame.

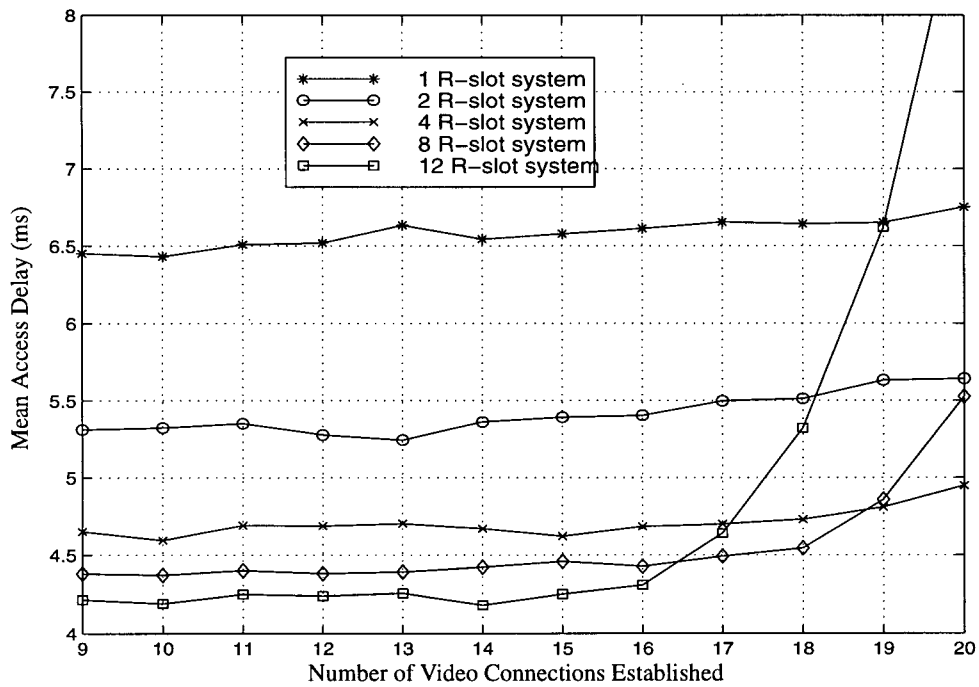

Figure 4.4. Mean Access Delay of Video Sources Under Low Traffic-load Condition.

It should be noted that when there are less than 15 video connections established in the ATDMA system, the traffic-load is extremely light since the base station can guarantee that I-slots are always available to fulfill the transmission rate requirements of the video sources. For instance, in the worst situation in which 15 video connections are transmitting simultaneously using the highest transmission rate class (class 3, which requires 4 I-slots per transmission frame

for each connection), a total number of 60 I-slots are needed to be allocated to the sources. Even in the 12 R-slot system in which 12 of the 72 time-slots per transmission frame are used for the reservation and acknowledgment purposes, the 60 I-slots requirement can be met. Figure 4.4 indicates that, when the number of video connections is less than 17, the access delay decreases as the number of R-slots per transmission frame increases, but remains almost constant with traffic load for a given number of R-slots per transmission frame. When the number of video connections is less than 17, the access delay of the video sources depends mainly on the response time of the base station, thus, using more R-slots per transmission frame can reduce the response time which results in a lower access delay. However, as shown in Figure 4.4, the access delay of the 12 R-slot, 8 R-slot, and the 4 R-slot systems start increasing as the number of video connections increases beyond 17. Figures 4.5 and 4.6 show the access delay of the video service when the number of video connections established in the system is increased to 28.

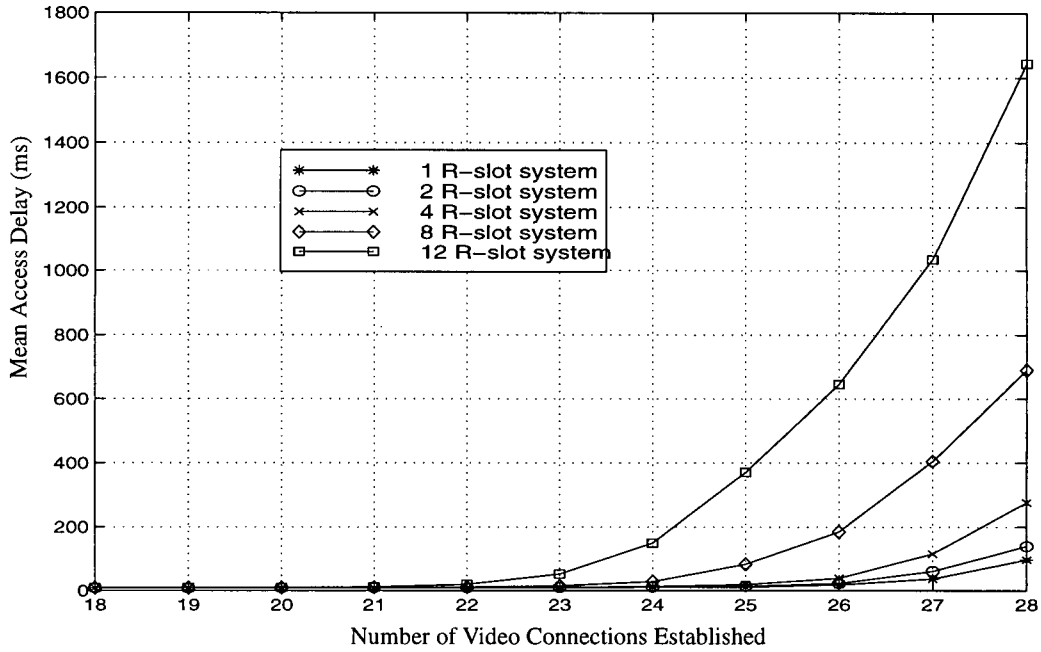

Figure 4.5. Mean Access Delay of Video Sources Vs. Number of Video Connections.

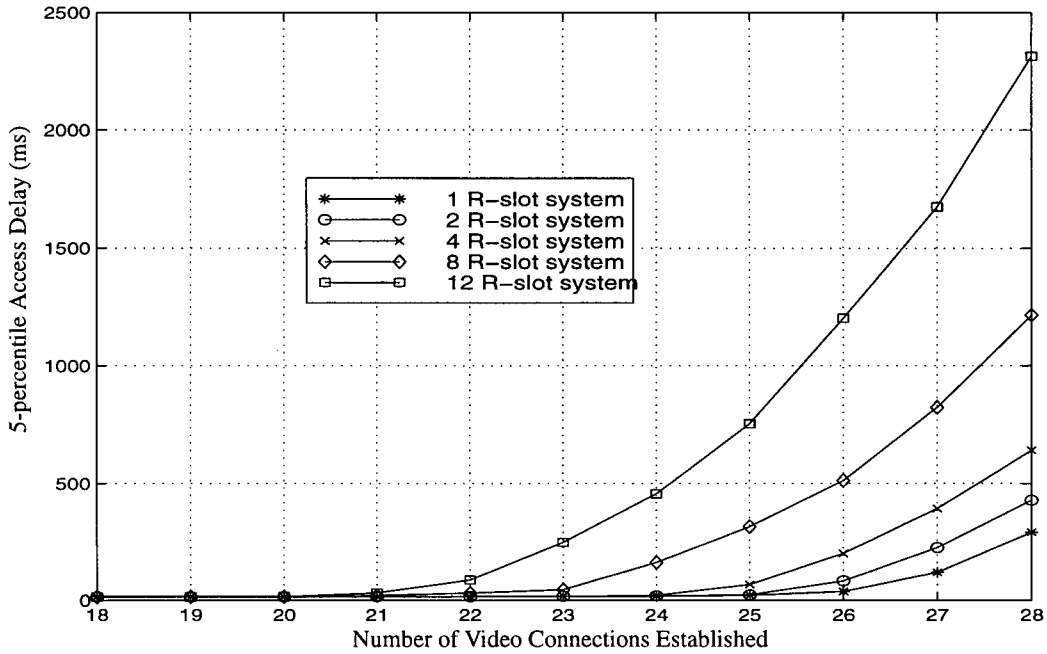

Figure 4.6. 5-percentile Access Delay Vs. Number of Video Connections.

As traffic-load increases, the number of free I-slots which can be allocated to I-slot requests decreases; therefore, video sources need to wait longer in the I-slot allocation queue for free I-slots. The queueing delay for free I-slots has become the main cause of the access delay experienced by video sources as traffic-load increases. Furthermore, Figures 4.5 and 4.6 indicate that a system using more R-slots per transmission frame has a higher access delay than a system using fewer number of R-slots as traffic-load increases. As described earlier, using more R-slots per transmission frame can shorten the response time of the base station by allowing it to make more I-slot allocations within a transmission frame. However, since the total number of time-slots per transmission frame is fixed at 72 slots in the ATDMA system, the number of R-slots per transmission frame can only be increased at the expense of reducing the number of I-slots. A reduction in the response time by using more R-slots per transmission frame will further reduce the availability of free I-slots as traffic-load increases. As a result, when traffic-load increases, video sources in the ATDMA system using more R-slots per transmission frame has a longer queueing delay for free I-slot when compared to a system using a fewer number of R-slots per transmission frame.

4.3 Video Packet Dropping Probability of Video Service using the Modified ATDMA Access Mechanism

In this thesis, an access delay threshold of 10 ms is applied to video service. Video sources drop the packets which cannot be transmitted in the I-slots within 10 ms after the end of a video frame. Furthermore, a 3% video packet dropping probability is assumed as a threshold for the first video frame after a video source switches to a higher transmission rate class. In order to calculate the video packet dropping probability (P_d), the fraction of the first video frame (after rate class increase of a video terminal) that is dropped due to violation of the 10 ms access delay threshold

is calculated using Equation 4.3.

$$F_d = \text{Fraction of packets dropped in the 1st video frame after rate increase}$$
$$= \frac{\text{No. of packets dropped in the 1st video frame}}{N_p} \tag{4.3}$$

where

$$N_p = \text{Number of video packets generated per video frame}$$
$$= \begin{cases} 39 \text{ packets}, & \text{rate class \#2} \\ 52 \text{ packets}, & \text{rate class \#3} \end{cases}$$

The packet dropping probability, P_d, is then obtained by averaging the value F_d calculated in the simulation. Figure 4.7 shows the probability, P_d, when different numbers of R-slot per transmission frame are used in the ATDMA system.

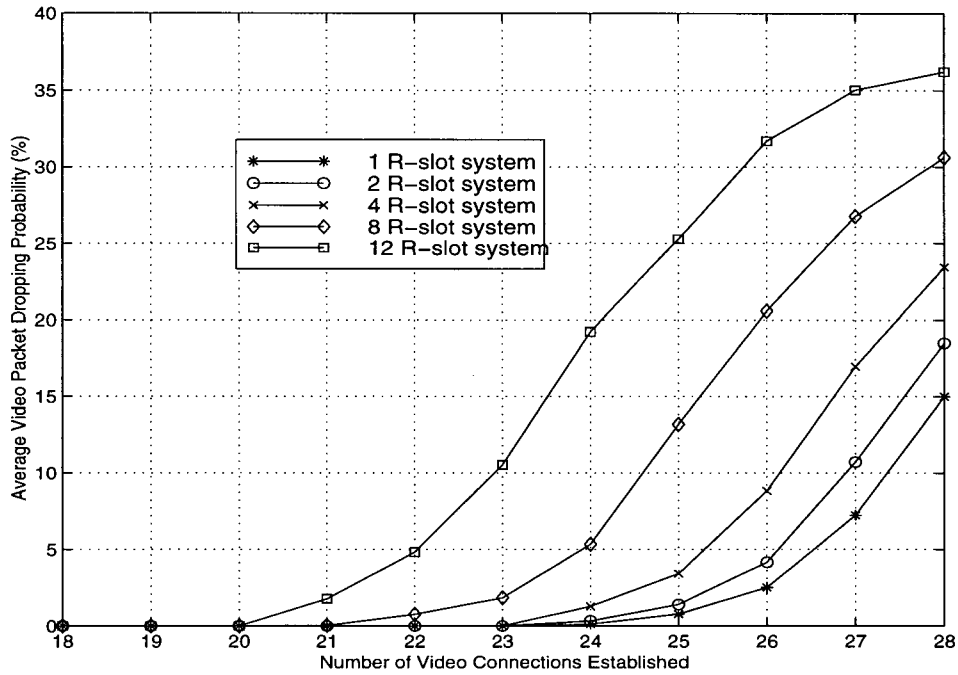

Figure 4.7. Average Video Packet Dropping Probability Vs. Number of Video Connections.

Figure 4.7 shows that the video packet dropping probability is almost 0% in all the ATDMA systems being investigated when the number of video connections established is less than 21. When the number of video connections increases beyond 21, the access delay of video sources increases (as shown in Figures 4.5 and 4.6); therefore, a larger number of video packets needed to be dropped because they cannot meet the 10 ms delay threshold. It is also observed that a system using more R-slots per transmission frame has a higher packet dropping probability when compared to a system using fewer number of R-slots. This result is expected because the video terminals need to stay longer in the I-slot allocation queue for free I-slot in those systems using more R-slots per transmission frame. Moreover, the probability P_d appears to level off at approximately 36% when there are 28 video connections established in the 12 R-slot ATDMA

system (an example of an extremely heavy traffic-load situation). Figure 4.8 is a histogram which shows the distribution of the access delay when there are 28 video connections established in the 12 R-slots ATDMA system.

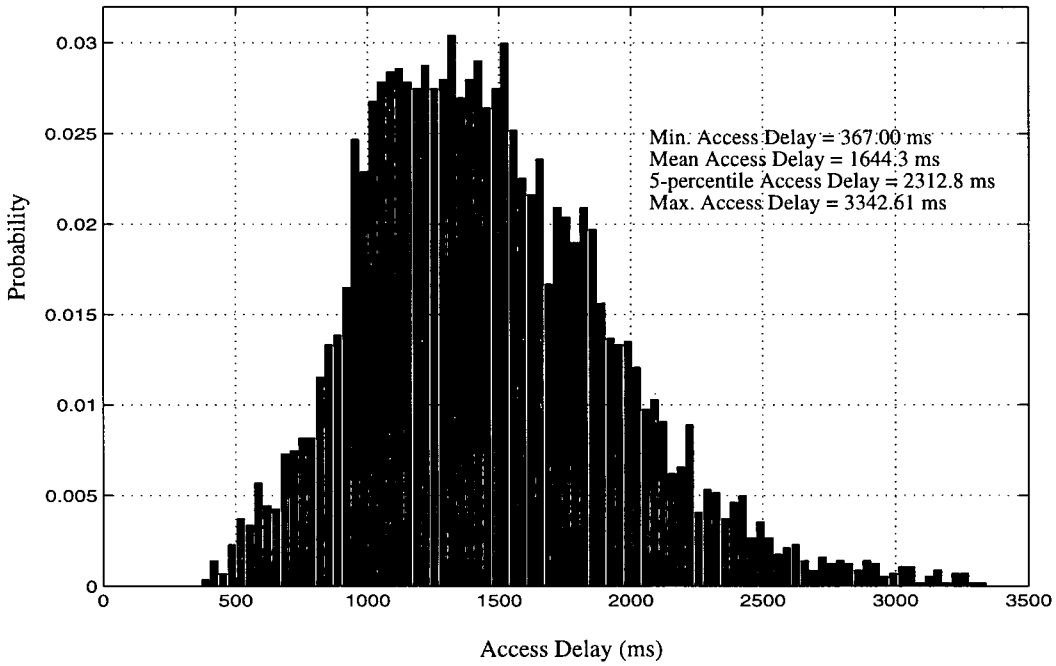

Figure 4.8. Distribution of the Access Delay (28 video connections established in the 12 R-slot syste

In Figure 4.8, it is observed that video sources experience a very high access delay when compared to the 5-percentile access delay threshold of 76.7 ms. In such a condition, a large number of video packets required to be transmitted by the extra I-slots are dropped due to excessive access delay.

In order to understand why the video packet dropping probability saturates at approximately 36-37% as traffic load increases, the extremely heavy traffic-load condition needs to be studied in more detail. Assuming that under an extremely heavy traffic-load condition, there is no

free I-slot available to be allocated to all I-slot requests from the video sources. Eventually, the video connections will be forced to transmit using transmission rate class #1 (the lowest transmission rate class which requires 2 I-slots per transmission frame). Therefore, all the video packets required to be carried by the extra I-slots are dropped due to excessive access delay. Under the extremely heavy traffic-load condition, the video dropping probability, $P_{d(\text{heavy})}$, of the first video frames after video sources switch to higher transmission rate classes can be estimated using Equation (4.4) and Equation (4.5). First, Equation (4.4) calculates the probability of rate class transition from class 1 to 2, $\text{Pr}_{(1\rightarrow 2)}$, and from class 2 to 3, $\text{Pr}_{(2\rightarrow 3)}$, given a rate class increase has occurred. In Equation 4.4, $\mu'(i)$ denotes the equilibrium probability of rate class i while P'_{ij} denotes the transition probability from class i to j. The values and derivation of $\mu'(i)$ and P'_{ij} can be found in Equation (3.5) to (3.12) of Chapter 3.

$$
\begin{aligned}
\text{Pr}_{(1\rightarrow 2)} &= \text{Pr}\ \{\text{class 1 to 2} \mid \text{rate class transition occurs}\} \\
&= \frac{\mu'(1)\cdot P'_{12}}{[\mu'(1)\cdot P'_{12}] + [\mu'(2)\cdot P'_{23}]} \\
&= 0.777 \\
\text{Pr}_{(2\rightarrow 3)} &= \text{Pr}\ \{\text{class 2 to 3} \mid \text{rate class transition occurs}\} \\
&= \frac{\mu'(2)\cdot P'_{23}}{[\mu'(1)\cdot P'_{12}] + [\mu'(2)\cdot P'_{23}]} \\
&= 0.223
\end{aligned}
\tag{4.4}
$$

Since each I-slot assigned to a video source can transmit 13 video packets per video frame, under the extremely heavy traffic-load condition, video sources requiring transmission rate class #2 (i.e. requiring 3 I-slots per transmission frame) will have 13 video packets dropped per video frame. Similarly, video sources requiring transmission rate class #3 (which require 4 I-slots per transmission frame) will have 26 video packets dropped per video frame. Equation 4.5 calculates

the average video packet dropping probability, $P_{d(\text{heavy})}$, of the first video frames after rate class increase under the extremely heavy load condition.

$$P_{d(\text{heavy})} = \left\{ \Pr_{(1 \to 2)} \cdot \left(\frac{13}{NP_2} \right) + \Pr_{(2 \to 3)} \cdot \left(\frac{2 \times 13}{NP_3} \right) \right\} \times 100\ \% \tag{4.5}$$

Where

NP_2 = 39 video packets generated per video frame (rate class 2)
NP_3 = 52 video packets generated per video frame (rate class 3)

Substituting the values of $\Pr_{(1 \to 2)}$ and $\Pr_{(2 \to 3)}$ into Equation (4.5), a $P_{d(\text{heavy})}$ of 37.05% is obtained. Therefore, as traffic-load increases, 37.05% is the expected upperbound of the average video packet dropping probability of the first video frames after video sources switch to higher transmission rate classes.

4.4 Performance Measures

Table 4.1 below shows the maximum number of video connections (N_{max}) that can be supported in the ATDMA systems (using different number of R-slots per transmission frame) which satisfy the following two QoS requirements:

(i) A 3% average video packet dropping probability of the first video frames after video sources increase their transmission rate classes.

(ii) A maximum 5-percentile access delay of 76.7 ms.

Table 4.1 Capacity of Various ATDMA systems and the Associated QoS

Number of R-slots per Transmission Frame	N_{max} and the Associated QoS Achieved			
	N_{max}	Av. Packet Dropping Probability (%)	Mean Access Delay (ms)	5-Percentile Access Delay (ms)
1	26	2.51	17.01	66.53
2	25	1.39	12.57	39.12
4	24	1.27	12.35	37.67
8	23	1.93	14.40	46.51
12	21	1.76	13.56	42.15

Table 4.1 shows that as the number of R-slots per transmission frame increases, the number of video connections which satisfy both the QoS requirements decreases. The maximum number of video connections that can be supported in the ATDMA system without violating the QoS requirements is 26 connections when 1 R-slot is used per transmission frame. Under this traffic-load condition, the QoS parameters achieved are: average video packet loss is 2.51%, mean access delay is 17.01 ms and the 5-percentile access delay is 66.53 ms. Figure 4.9 shows a histogram of the access delay when there are 26 video connections established in the 1 R-slot system.

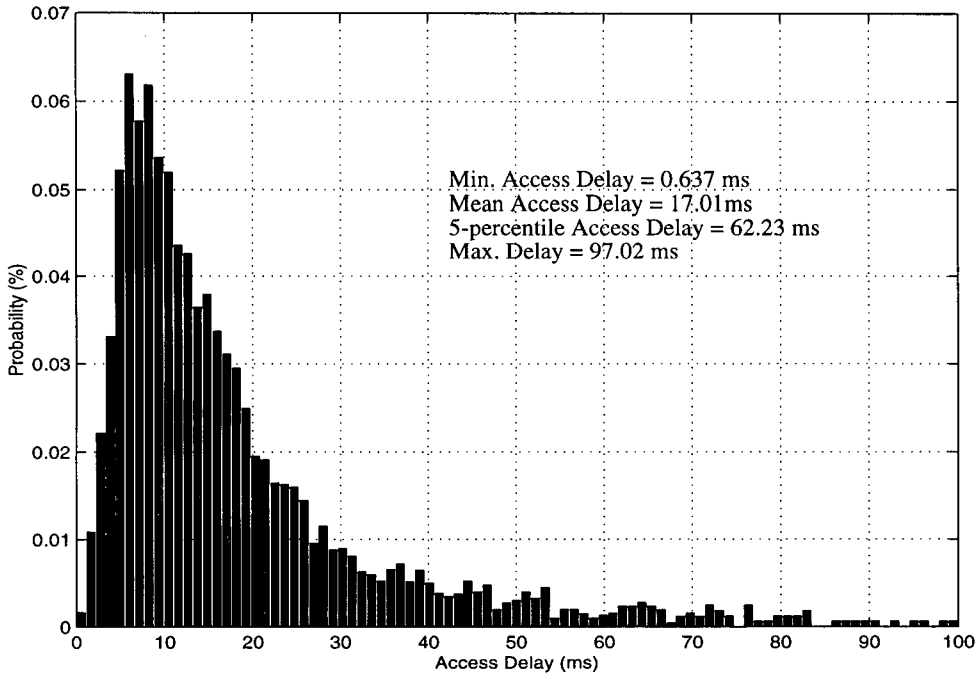

Figure 4.9. Distribution of the Access Delay (26 video connections established in the 1 R-slot system

In order to evaluate the effectiveness of the dynamic bandwidth assignment strategy proposed in the modified ATDMA access mechanism, it is useful to compare N_{max} to the maximum number of video connections which can be established using the original ATDMA access mechanism proposed in [5] in which a fixed amount of bandwidth is assigned to each connection during its period of activity. When the access mechanism in [5] is used, the base station must assign 4 time-slots per transmission frame to each video connection in order to fulfill the maximum bit-rate requirement of the modified H.261 video codec. In the ATDMA system which uses a 72 time-slot TDMA frame structure, the fixed bandwidth assignment strategy can support a maximum of 18 video connections ($\frac{72 \text{ slots}}{4 \text{ slots/ connection}} = 18$ connections). Column 3 of Table 4.2 shows the percentage increase in capacity when the dynamic bandwidth assignment

strategy proposed in this thesis is compared to the fixed bandwidth assignment strategy used in [5]. It is observed that the dynamic bandwidth assignment strategy used in the modified access mechanism can allow a maximum capacity increase of 44.4% (using the 1 R-slot ATDMA system) when compared to the fixed bandwidth assignment strategy.

Table 4.2 Performance Evaluation of the Modified ATDMA Access Mechanism

Number of R-slots per Transmission Frame	N_{max}	Capacity increase $= \left(\frac{N_{max} - 18}{18} \cdot 100\%\right)$	N_{max}'	Efficiency
1	26	44.4%	28	92.8%
2	25	38.9%	27	92.6%
4	24	33.3%	26	92.3%
8	23	27.7%	25	92.0%
12	21	16.7%	23	91.3%

Column 4 of Table 4.2 displays the maximum number of video connections (N_{max}') that can be supported using the modified ATDMA access mechanism under an ideal situation in which the dynamic sharing of I-slots between different video connections is in perfect synchronization. The number N_{max}' of Table 4.2 can be estimated by first calculating an effective transmission rate for each video connection (*Eff_rate*), defined as the average number of I-slots per transmission frame required by a VBR video connection.

$$\begin{aligned} Eff\_rate &= \mu'(1) \cdot 2 + \mu'(2) \cdot 3 + \mu'(3) \cdot 4 \\ &= 2.535 \text{ (I-slots/transmission frame)} \end{aligned} \tag{4.6}$$

where

$\mu'(1)$ = Equilibrium probability of rate class 1 = 0.499
$\mu'(2)$ = Equilibrium probability of rate class 2 = 0.467
$\mu'(3)$ = Equilibrium probability of rate class 3 = 0.034

N_{max}' can then be calculated using Equation 4.7:

$$N_{max}' = \left\lfloor \frac{N_T - N_R}{Eff\_rate} \right\rfloor \tag{4.7}$$

where

N_T = Number of time-slots per transmission frame = 72
N_R = Number of R-slots per transmission frame

The last column of Table 4.2 evaluates the efficiency of the proposed access mechanism when compared with the ideal situation in which perfect synchronization is assumed in the dynamic sharing of I-slots between different video sources. The efficiency is calculated as follows:

$$\text{Efficiency} = \left(\frac{N_{max}}{N_{max}'}\right) \times 100\ \% \tag{4.8}$$

From the results in Table 4.2, it is observed that the efficiency of the modified ATDMA access mechanism is higher in those systems using a fewer number of R-slots per transmission frame. For instance, when the 1 R-slot ATDMA system, a maximum efficiency of 92.8% can be achieved.

Chapter 5 Performance Evaluation of Mixed Voice and Video services

In this chapter, we examine the performance of the modified ATDMA access mechanism in supporting mixed voice and video services. The access delay and packet dropping probability of the voice and video services are examined under different traffic-load conditions. Furthermore, the effects on the performance when different priorities in accessing channels for voice and video services are also investigated.

5.1 Performance Analysis of Mixed Voice and Video Services Under Different Traffic-load Conditions

In this section, the quality of service (QoS) of the mixed traffic (i.e. the access delay and the packet dropping probability) is evaluated under various traffic-load conditions. Moreover, the performance of the modified access mechanism is compared to that of the access mechanism proposed in [5].

The voice and video services are given the same priority in accessing channels in this section. In Section 5.2, an access scheme which assigns different priorities to the voice and video services is examined. The specifications of the voice and video source models are outlined in Section 2.3.1 of Chapter 2 and in Section 3.2.3 of Chapter 3, respectively. A 4 R-slot ATDMA system is chosen because, for voice service, using less than 4 R-slots per transmission frame may trigger the occurrence of multiple collisions of reservation requests in the R-slots even under low traffic-load conditions. For instance, in the 3 R-slot system, multiple collisions occur which cause excessive contention delay when the number of voice connections increases beyond 115 (as a comparison, as shown in Chapter 2, a maximum of 140 voice connections can be supported in the

4 R-slot ATDMA system). The excessive contention delay eventually leads to a significant quality degradation of voice traffic.

This section studies the performance of the access mechanism under a variety of voice and video traffic-load combinations. First, the performance of the access mechanism is evaluated when there are 10 video connections established simultaneously with varying levels of voice traffic. Next, there is a study on the performance of other scenarios in which different numbers of video connections are established together with varying levels of voice traffic. Finally, there is a performance assessment of the proposed access mechanism in supporting mixed voice and video services based on the simulation results.

In the following discussion, two conventions are used to display the simulation results. "Access mechanism (a)" refers to the access mechanism proposed in [5] which uses a fixed bandwidth assignment strategy during the activity period of a connection. "Access mechanism (b)" refers to the modified access mechanism proposed in this thesis which uses a dynamic bandwidth assignment strategy to allocate bandwidth to a connection on a demand basis.

5.1.1 Performance Evaluation of the 10 Video Connection Scenario

In this scenario, 10 video connections are established together with varying levels of voice traffic in the ATDMA system. Figures 5.1 and 5.2 show the access delay and packet dropping probability (as defined in Sections 4.1 and 4.3, respectively) of the voice traffic, respectively.

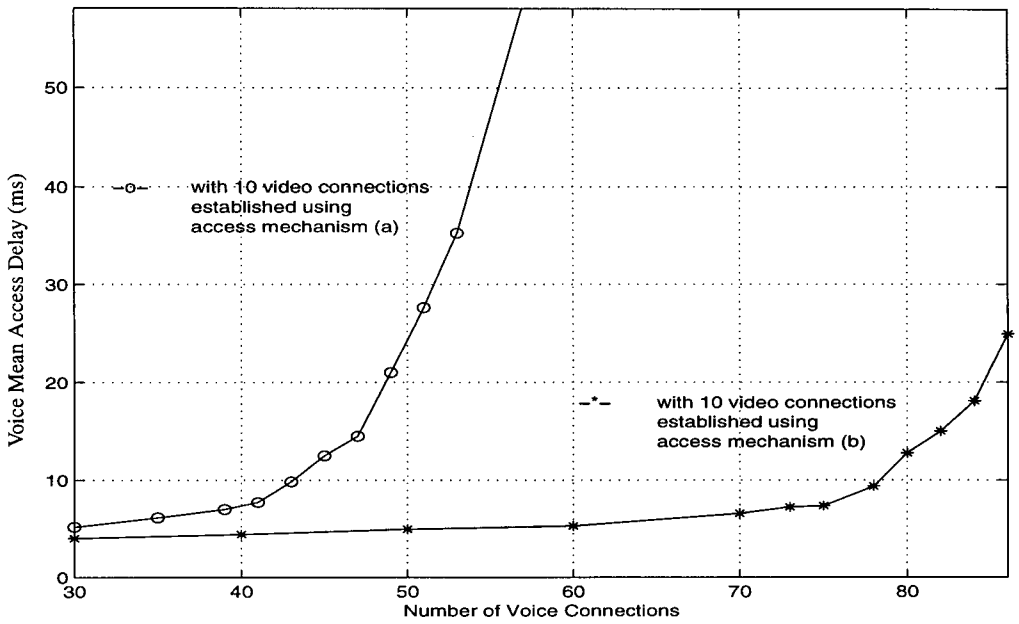

Figure 5.1. Access delay of Voice Traffic - 10 Video Connections

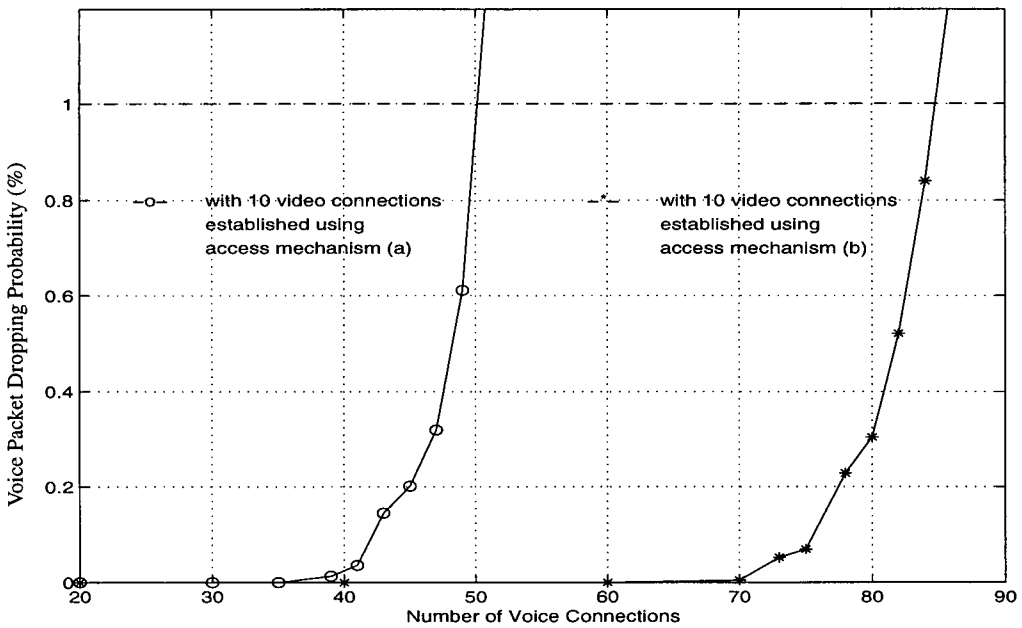

Figure 5.2. Packet Dropping Probability of Voice Traffic - 10 Video Connections Established.

Figure 5.1 shows that for both access mechanisms, the access delay of the voice traffic increases with the number of voice connections established in the system. This result is expected since the increased number of voice connections results in a higher demand for free I-slots; therefore, voice terminals need to wait longer in the I-slot allocation queue for I-slot assignments. Figure 5.1 also shows that, under the same traffic-load condition, the system using access mechanism (b) has a lower access delay when compared to the system using access mechanism (a). In access mechanism (b), the base station allocates I-slots to video terminals on a demand basis. Since the video traffic exhibits variable bit-rate (VBR) characteristics, the base station assigns a fewer number of I-slots to the video terminals during their periods of low activity. This results in more I-slots being available for allocation to voice terminals, which eventually leads to a decrease in access delay of voice traffic.

Figure 5.2 shows the packet dropping probability of the voice traffic. From Figure 5.2, we can observe the following characteristics as the number of voice connections increases:

(i) The voice packet dropping probability of both access mechanisms increases with the number of voice connections. As the number of voice connections increases, the higher access delay experienced by voice terminals causes more packets to be dropped due to violation of the 10 ms voice packet access delay threshold.

(ii) When access mechanism (a) is used, the voice packet dropping probability is almost negligible when there are less than 35 voice connections established. However, the packet dropping probability starts increasing significantly when the number of voice

connections increases beyond 40. By assuming a threshold of 1% voice packet dropping probability, the system using access mechanism (a) can at most support 50 voice connections.

(iii) The access mechanism (b) gives a negligible voice packet dropping probability when the number of voice connections is below 65. The packet dropping probability starts increasing significantly when the number of voice connections increases beyond 70. The 1% voice packet dropping probability threshold is reached when there are 85 voice connections established in the system. Therefore, when compared to access mechanism (a), the system using access mechanism (b) can increase the voice traffic capacity from 50 to 85 connections when there are 10 video connections established in the system. However, the presence of the voice traffic may affect the QoS of the 10 video connections established in the system. This area is to be studied next.

The disadvantage of using access mechanism (b) in supporting video traffic is that the dynamic bandwidth assignment strategy cannot always guarantee the allocation of sufficient bandwidth to video connections (as opposed to the fixed bandwidth assignment strategy used in access mechanism (a)). During the low-activity periods of a connection, video terminals allow other terminals (voice and video terminals) to use the surplus I-slots that would otherwise remain reserved in the fixed bandwidth assignment strategy. Whenever a low-activity video terminal switches to a higher-activity level (i.e. increases its transmission rate class), it must reclaim the I-slots that it has released to the base station during the low-activity period. As illustrated in Chapter 3, after video terminals send I-slot requests through in-band signalling, there is an access delay before they can start transmission in the extra I-slots allocated by the base station. As the traffic load of the system increases, access delay increases since video terminals need to wait

longer in the I-slot allocation queue for free I-slots. As a result, video packets will be dropped if they cannot be delivered by the extra I-slots within a 10 ms access delay threshold for video service. Figures 5.3 and 5.4 shows the performance of access mechanism (b) in supporting the 10 video connections under varying levels of voice traffic.

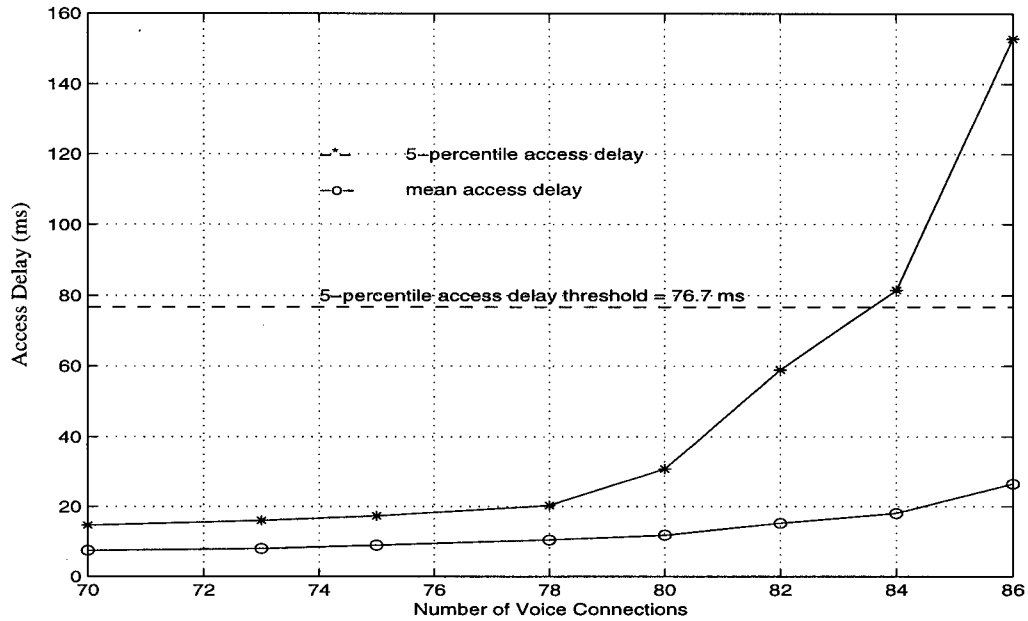

Figure 5.3. Access Delay of Video Traffic - 10 Video Connections Established

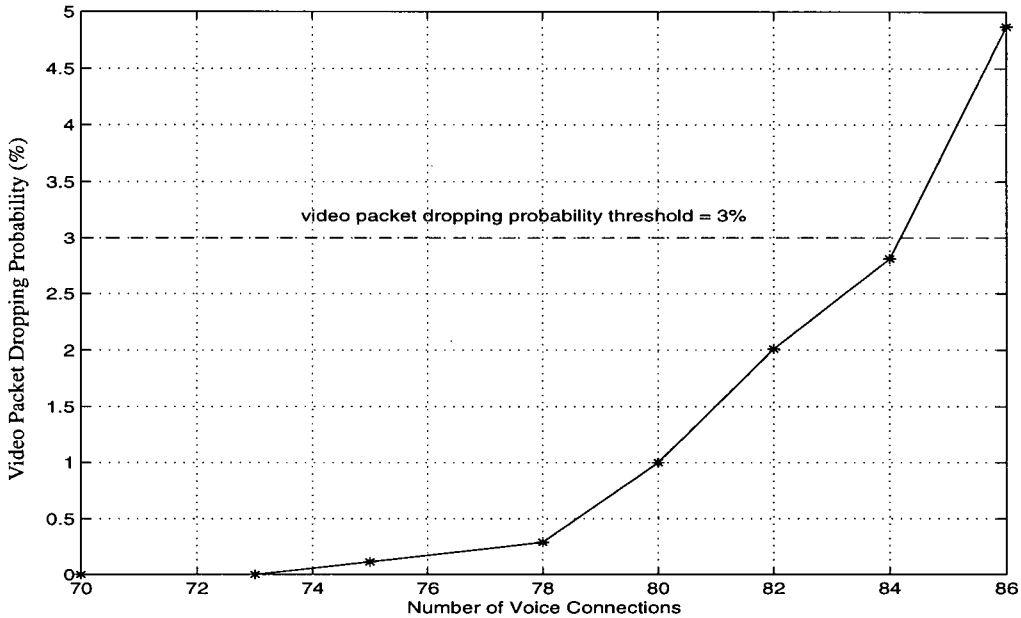

Figure 5.4. Packet Dropping Probability of Video Traffic - 10 Video Connections Established

In the figures, we can observe the following three characteristics.

(i) The access delay experienced by video terminals increases with the number of voice connections. As the number of voice connections established in the system increases, the higher demand for I-slots causes the video terminals to wait longer in the I-slot allocation queue which results in a higher access delay.

(ii) As the number of voice connections established increases, the increasing access delay of video traffic causes more video packets to be dropped due to violation of the 10 ms access delay threshold. Therefore, the packet dropping probability rises accordingly.

(iii) As observed in Figure 5.2 earlier, a maximum number of 85 voice connections can satisfy the 1% packet dropping probability threshold of voice service when there are 10 video connections established using the access mechanism (b). However, in a system using access mechanism (b), there is a mutual interaction in the dynamic sharing of I-slots between the voice and video services (as opposed to the access mechanism (a) in which video connections are established in a connection oriented manner, thus, there is no interaction between the voice and video services). Therefore, in a system which uses access mechanism (b), the presence of voice traffic may affect the QoS of the video traffic, and vice-versa. When the 3% video packet dropping probability and the 5-percentile access delay of 76.7 ms are applied together as thresholds for the 10 video connections established, Figures 5.3 and 5.4 show that the maximum number of voice connections that can be accommodated together with the video traffic must be lowered from 85 to 83 connections. Therefore, when compared to the maximum number of 50 voice connections that can be supported using access mechanism (a), the access mechanism (b) can achieve an increase in voice traffic capacity of 66% (i.e $\frac{(83-50)}{50} \times 100\,\% = 66\%$).

5.1.2 Studies of Other Voice and Video Traffic-load Combination Scenarios and Performance Measures

In this section, the performances of access mechanisms (a) and (b) in supporting mixed traffic are further studied under different voice and video traffic-load combinations. First, Figures 5.5 to 5.8 show the access delays and packet dropping probabilities of the mixed traffic when there are 5 and 15 video connections established together with varying levels of voice traffic.

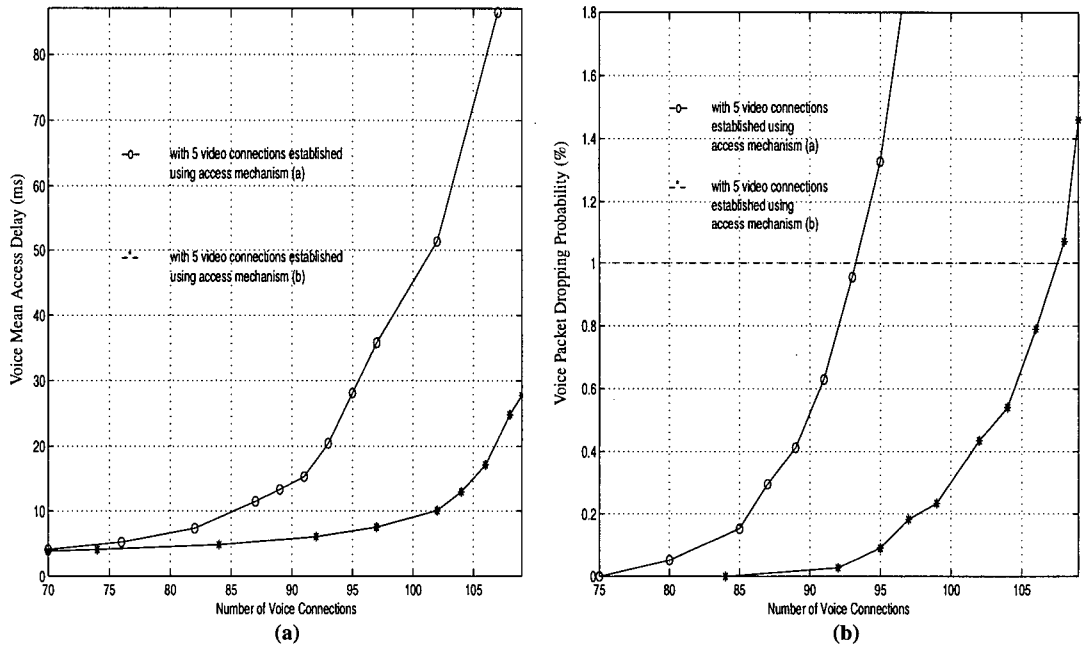

Figure 5.5. QoS of the Voice Traffic - 5 Video Connections Established

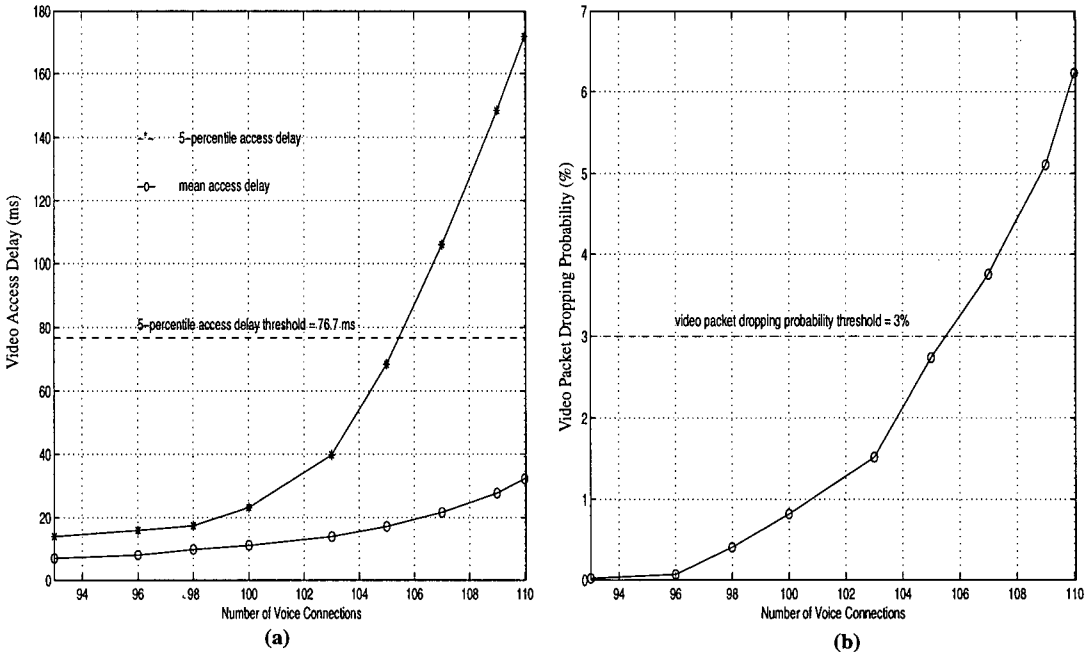

Figure 5.6. QoS of the Video Traffic - 5 Video Connections Established

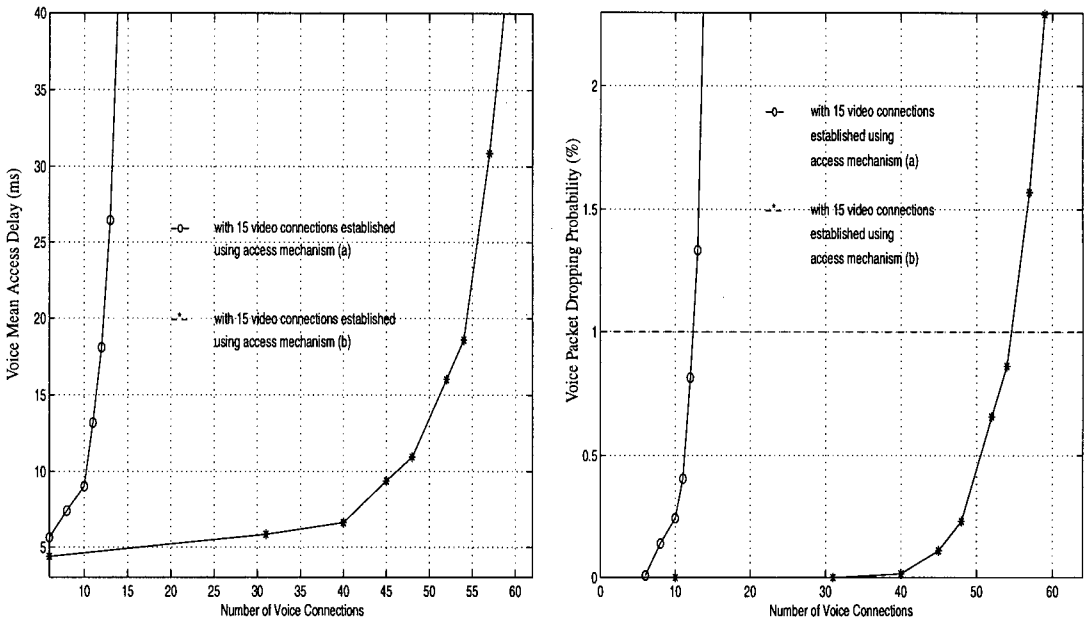

(a) (b)

Figure 5.7. QoS of the Voice Traffic - 15 Video Connections Established

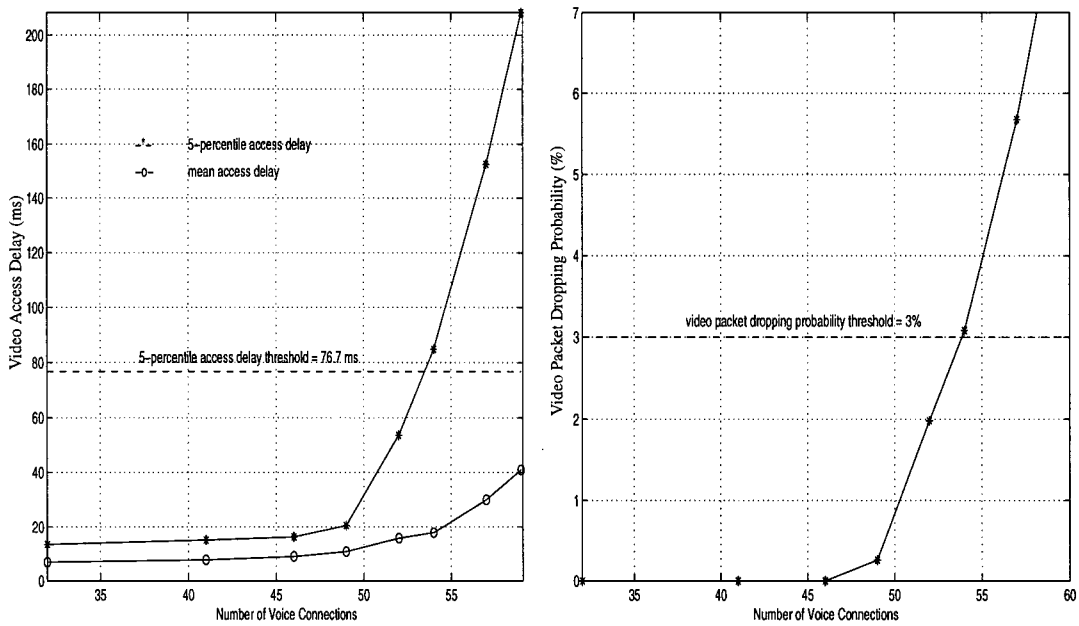

(a) (b)

Figure 5.8. QoS of the Video Traffic - 15 Video Connections Established.

From Figures 5.5 to 5.8, the following characteristics can be observed:

(i) Figure 5.5 shows that, under the same traffic-load condition, access mechanism (b) can maintain a lower access delay when compared to access mechanism (a). When the 1% packet dropping probability is applied as threshold to both access mechanisms, access mechanism (a) can at most support 93 voice connections while access mechanism (b) can increase the capacity to 107 connections.

(ii) Figures 5.6 shows the effects of varying levels of voice traffic on the performance of the 5 video connections established in the system when access mechanism (b) is used. In access mechanism (b), there is a dynamic sharing of free I-slots between voice and video services. Hence, the presence of one traffic may affect the QoS of the other traffic. From Figures 5.6 (a) and (b), it is observed that if the video QoS requirements (i.e. 3% packet probability and a maximum 5-percentile access delay of 76.7 ms) are to be respected simultaneously, the maximum number of voice connections that can be accommodated together with 5 video connections must be lowered to 105 (instead of the 107 connections as observed in Figure 5.6 (b)).

(iii) Figures 5.7 and 5.8 show similar characteristics as observed in Figures 5.5 and 5.6. Figure 5.7 shows that, when 15 video connections are established in the system, a maximum of 12 voice connections can be established using access mechanism (a) while satisfying the 1% packet dropping probability limit. However, when access mechanism (b) is used, the voice traffic capacity can be increased to 54 connections. Figure 5.8 shows that, when access mechanism (b) is used, the presence of 54 voice connections degrades the QoS of the video traffic to such an extent that both the 5-percentile access

delay and the 3% packet dropping probability thresholds are violated. In order to respect all the QoS requirements of the voice and video services simultaneously, the maximum voice traffic capacity must be lowered from 54 to 53 voice connections.

By establishing different numbers of video connections in the system and evaluating the performance of the access mechanisms under varying voice traffic load conditions, the acceptable traffic-load curves for access mechanisms (a) and (b) can be obtained, as shown in Figure 5.9.

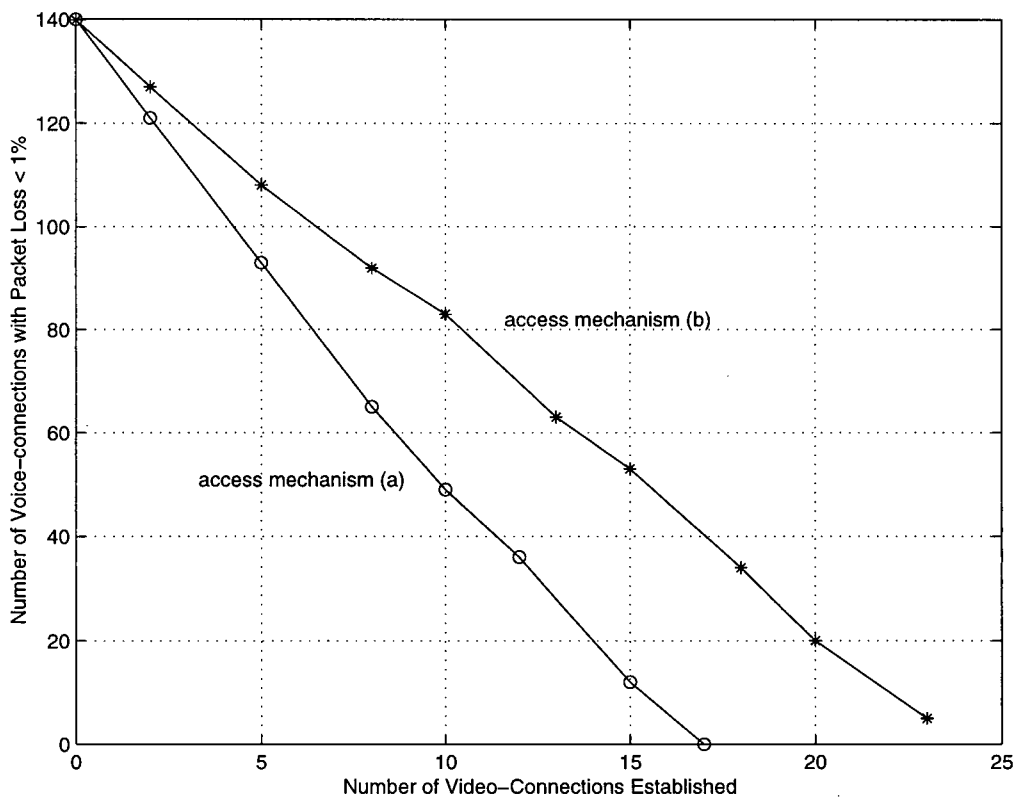

Figure 5.9. Acceptable Traffic-load Curves for Access Mechanisms (a) and (b).

In Figure 5.9, the maximum acceptable voice traffic-load is plotted as a function of the number of video connections established in the ATDMA system. The areas under the two curves

represent the acceptable-load regions for the system using access mechanism (a) and (b), respectively. From Figure 5.9, it is observed that, when compared to access mechanism (a), the system using access mechanism (b) can accommodate a higher number of voice connections under a given level of video traffic. The system using access mechanism (b) can achieve a higher voice traffic capacity because the dynamic bandwidth assignment strategy used is more efficient and flexible in allocating bandwidth (in number of I-slots/transmission frame) to different terminals on a demand basis. Since the video traffic exhibits variable-bit-rate (VBR) characteristics, access mechanism (b) retrieves the surplus I-slots from video terminals during their low-activity periods and re-allocates the I-slots to other terminals (voice and video terminals) waiting in the I-slot allocation queue. Hence, under the same traffic-load condition, the system using access mechanism (b) can always maintain a larger pool of free I-slots that is available to be shared dynamically among terminals.

In order to assess the performance of the access mechanisms (a) and (b), it is useful to compare the efficiency of the two access mechanisms to an ideal situation in which the dynamic sharing of I-slots among voice and video terminals is in perfect synchronization. Assuming $N_{max}(j)$ be the maximum number of voice connections that can be accommodated together with j video connections under the ideal situation. The number $N_{max}(j)$ can be estimated using the effective transmission rate of the video terminal (Eff_rate = 2.535 I-slots/transmission-frame as calculated in Equation 4.6 of Chapter 4) and the effective duty-cycle (Eff_duty) of the voice source. The effective duty cycle of the voice source is calculated as follows:

$$Eff\_duty = \frac{T_{act}}{(T_{act} + T_{sil})} = 0.448 \tag{5.1}$$

where

T_{act} = mean talkspurt duration = 1.41 sec
T_{sil} = mean silence duration = 1.74 sec

When there are j video connections established in the 4 R-slot ATDMA system (i.e 68 I-slots per transmission frame), the average number of free I-slots per transmission frame available for voice traffic (I_{vo}) can be estimated using Equation (5.2).

$$I_{vo} = 68 - Eff\_rate \times j \tag{5.2}$$

Next, Equation 5.3 can be used to estimate $N_{max}(j)$ as follows:

$$N_{max}(j) = \left\lfloor \frac{I_{vo}}{Eff\_duty} \right\rfloor \tag{5.3}$$

Finally, when there are j video connections established in the ATDMA system, the efficiency of the access mechanisms (a) and (b) when compared to the ideal situation can be calculated using Equation 5.4. In Equation 5.4, $N_a(j)$ and $N_b(j)$ denote the maximum number of voice connections that can be supported together with j video connections (without violating the QoS requirements for both voice and video services) using the access mechanism (a) and (b), respectively.

$$
\begin{aligned}
Eff_a(j) &= \left[\frac{N_a(j)}{N_{max}(j)}\right] \times 100\% \\
Eff_b(j) &= \left[\frac{N_b(j)}{N_{max}(j)}\right] \times 100\%
\end{aligned}
\tag{5.4}
$$

Figure 5.10 shows the efficiency of the access mechanism (a) and (b) as a function of the number of video connections established (i.e. j) in the ATDMA system.

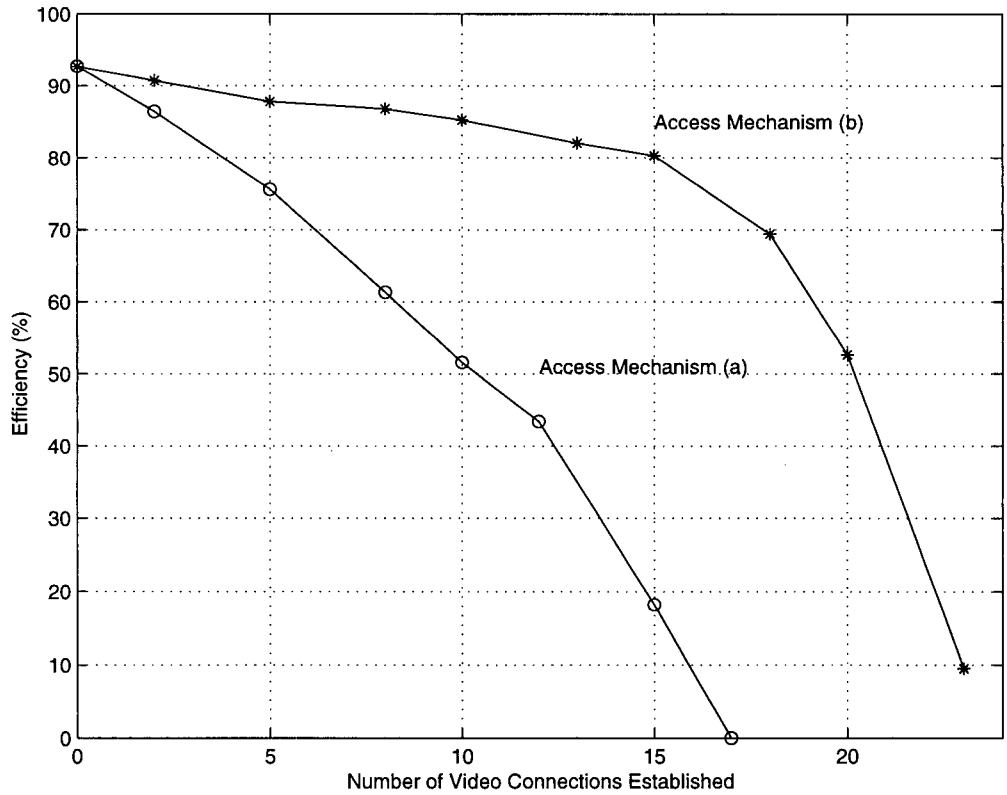

Figure 5.10. Efficiency of Access Mechanisms (a) and (b).

From Figure 5.10, we can observe the following characteristics:

(i) When there are no video connections established (i.e. $j = 0$), the system uses the access mechanism as described in Chapter 2 to support voice traffic. Since a maximum of 140 voice connections can be established while respecting the 1% packet dropping probability threshold, the system can achieve an efficiency of 92.7% (under perfect synchronization, $N_{max}(0) = 151$). Several factors account for the difference between the actual performance and the upperbound of 100% efficiency. First, the irregular patterns of talkspurt arrivals from voice terminals prevent the access mechanism from making a perfect schedule of I-slot assignments. Second, voice terminals suffer additional access delay when their reservation requests are involved in collisions occurred in the R-slots. Furthermore, after a collision, voice terminals enter the collision resolution phase and attempt retransmissions in the next available R-slot with a specified permission probability. Therefore, I-slots may be wasted if the terminals have voice packets to send but fail to obtain permission for the retransmission of reservation requests.

(ii) When compared to access mechanism (a), access mechanism (b) can achieve a higher efficiency under the same video traffic load condition. As previously discussed, the bandwidth assignment strategy used in access mechanism (b) is more flexible to alloacte I-slots to different terminals on a demand basis.

(iii) The efficiency of the two access mechanisms decreases as the number of video connections established in the system (i.e. j) increases. The efficiency of an access mechanism depends on the number of I-slots per transmission-frame that is available to be shared dynamically among terminals. As the number of free I-slots per transmission-frame in-

creases, more terminals can be supported together in the system. The higher number of terminals can, in turn, reduce the effects of the irregular pattern of reservation request arrivals in degrading the performance of the access mechanism. For instance, consider a period of time in which the I-slot request arrival rate is higher than average. The sudden increase in the demand for free I-slots may cause a significant QoS degradation since the system may not have sufficient I-slots to satisfy the requirement. However, as the number of terminals supported in the system increases, it is more likely that the arrival rate of reservation requests approaches an average (i.e. the numbers of simultaneous speakers and video terminals switching to higher transmission rate-classes are nearly average). As a result, the extent of quality degradation caused by the irregular pattern of I-slot request arrivals can be reduced. It should be noted that in both access mechanisms (a) and (b), as j increases, the number of I-slots per transmission-frame that is available for dynamic sharing among terminals decreases. For instance, in access mechanism (a) which assigns bandwidth to video traffic on a connection-oriented basis, each video connection will occupy 4 I-slots per transmission-frame that would, otherwise, be available for dynamic sharing among voice terminals. Similarly, in access mechanism (b), at least 2 I-slots per transmission-frame will be occupied by each video connection since the lowest transmission rate-class requires 2 I-slots per transmission-frame. Therefore, as j increases, the size of the I-slot pool that is available for dynamic sharing among terminals decreases in both access mechanisms. As a result, the fewer number of I-slots that can be shared dynamically among terminals causes the efficiencies of the two access mechanisms to decrease.

(iv) The efficiency of access mechanism (a) decreases at a faster rate when compared to access mechanism (b). For instance, when video traffic increases to 10 connections (i.e. $j = 10$), the efficiency of the system using access mechanisms (a) and (b) drops from the maximum of 92.7% to 52.6% and 87.4%, respectively. As discussed previously, the efficiency of an access mechanisms depends on the size of the I-slot pool that is available for dynamic sharing among terminals. As j increases, the size of the I-slot pool (for dynamic sharing) decreases at a rate of 4 I-slots per video-connection for access mechanism (a), and at a rate of 2 I-slots per video-connection for access mechanism (b). Therefore, as j increases, access mechanism (a) has a faster rate of decrease in the size of the I-slot pool which accounts for its faster rate of decrease in efficiency when compared to access mechanism (b).

5.2 Performance Analysis when Voice and Video Services are Assigned with Different Priorities in Accessing Channels

In this section, we attempt to further increase the capacity of the modified ATDMA access mechanism by assigning different priorities to the voice and video services in accessing channels. In order to choose a suitable priority assignment strategy, it is useful to study the QoS that the voice and video services achieve under different traffic-load conditions, when both services have the same priority in accessing channels. Table 5.1 shows a sample of the number $N_b(j)$ (i.e the maximum number of voice connections that can be accommodated together with j video connections when access mechanism (b) is used) and the associated QoS achieved by the voice and video

services.

Table 5.1 QoS of the Mixed Voice and Video Services (same priority)

Video Number (j)	QoS of Video and Voice Services				$N_{vo}(j)$	P_{diff} (%)
	$N_b(j)$	P_{vo} (%)	P_{vi} (%)	D_{vi} (ms)		
2	127	0.52	2.82	74.8	130	+2.4
5	105	0.67	2.74	68.2	107	+1.9
8	92	0.61	2.48	67.3	94	+2.2
10	83	0.72	2.43	69.7	85	+2.4
13	62	0.70	2.55	67.3	63	+1.6
15	53	0.76	2.61	70.2	54	+1.9
18	34	0.62	2.21	54.8	35	+2.9
20	25	0.85	2.36	60.2	25	0

In Table 5.1, the QoS parameters P_{vo}, P_{vi}, and D_{vi} denotes the voice packet dropping probability, video packet dropping probability and the 5-percentile access delay of video traffic, respectively. The number $N_{vo}(j)$ represents the maximum number of voice connections (without violating the 1% voice packet dropping probability threshold) that can be accommodated together with j video connections when voice and video services have the same priority in accessing channels. The last column shows the percentage difference between $N_{vo}(j)$ and $N_b(j)$ which is calculated as follows:

$$P_{diff} = \left(\frac{N_{vo}(j) - N_b(j)}{N_b(j)}\right) \times 100\ \% \tag{5.5}$$

From Table 5.1, it is observed that the number $N_{vo}(j)$ is greater than $N_b(j)$ in most cases. This observation indicates that, when voice and video services are given the same priority in accessing channels, video traffic has to meet more stringent QoS requirements when compared to

the voice traffic. For instance, when there are 10 video connections established (i.e. $j = 10$), a maximum of 85 voice connections can be established while still satisfying the 1% voice packet dropping probability threshold (i.e. $N_{vo}(10) = 85$). However, as shown in Figures 5.3 and 5.4, the presence of the 85 voice connections degrades the quality of the video traffic such that the QoS thresholds for the video service are violated. Therefore, the maximum voice traffic-load must be lowered from 85 to 83 connections (i.e. $N_b(10) = 83$) if the QoS thresholds for the voice and video services are to be respected simultaneously.

Based on Table 5.1, it can be seen that a capacity increase of at most 3% could be obtained by assigning a higher priority to video connections in accessing channels. Even though the potential increase in capacity is small, we will look at the effects of a simple priority scheme on capacity.

This section introduces a simple priority scheme which, under different traffic-load conditions, assigns to the video traffic an adjustable priority over the voice traffic in accessing channels. In the priority scheme, two separate I-slot allocation queues with different priorities are maintained for the reservation requests from voice and video services. When a free I-slot is available, the reservation requests waiting in the high priority queue will first be served. The reservation requests in the low priority queue will only be served when the high priority queue is empty. When a reservation request from a video terminal arrives, it will always be routed to the high priority queue. However, when a reservation request originated from a voice terminal arrives, it will be routed to the high priority queue with a probability of p (i.e. the probability that it will be routed to the low priority queue is $(1-p)$). Therefore, by varying the value of p, the degree of priority that the video traffic possesses over the voice traffic can be adjusted. For

instance, a lower value of p will cause a smaller number of voice traffic requests to enter the high priority queue; thus, the presence of the voice-traffic will have a smaller effect on the QoS of the video traffic (which always enter the high priority queue). Figure 5.11 illustrates the priority assignment scheme.

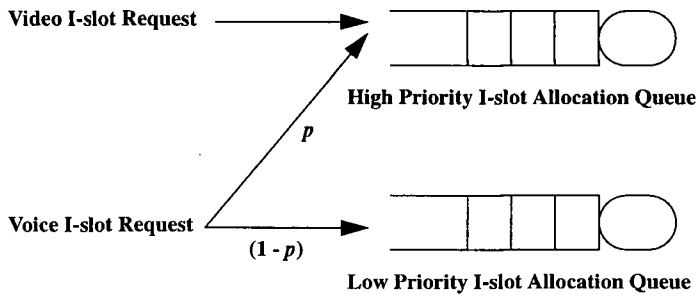

Figure 5.11. A Priority Assignment Scheme.

To assess the effectiveness of this scheme, first, the extreme situation in which the probability "p" is set to zero is studied. In this priority arrangement, all reservation requests from the video terminals will be routed to the high priority queue while all voice traffic reservation requests will be routed to the low priority queue. It is expected that the QoS of the video traffic will be improved since the access delay of the video traffic will not be affected by the number of voice terminals waiting in the low priority I-slot allocation queue. However, the QoS of the voice traffic will be degraded since the requests of the voice traffic will only be served when the high priority queue is empty. In the following performance evaluation, "access mechanism (c, p)" refers to the modified ATDMA access mechanism with the additional feature that the priority scheme as illustrated in Figure 5.11 is applied (the variable "p" represents the routing probability for the voice traffic). Figures 5.12 and 5.13 show the effects of varying levels of voice traffic on the QoS of 5 and 15 video connections when access mechanism (c, p=0) is used.

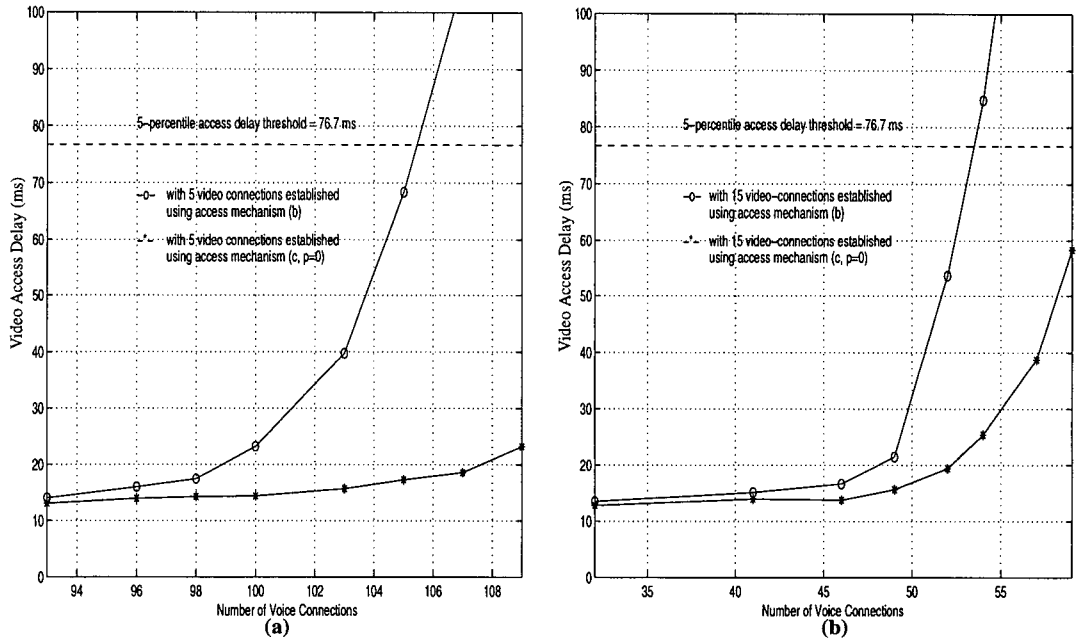

Figure 5.12. Access Delay of Video Traffic When Access Mechanism (c, *p*=0) is Applied

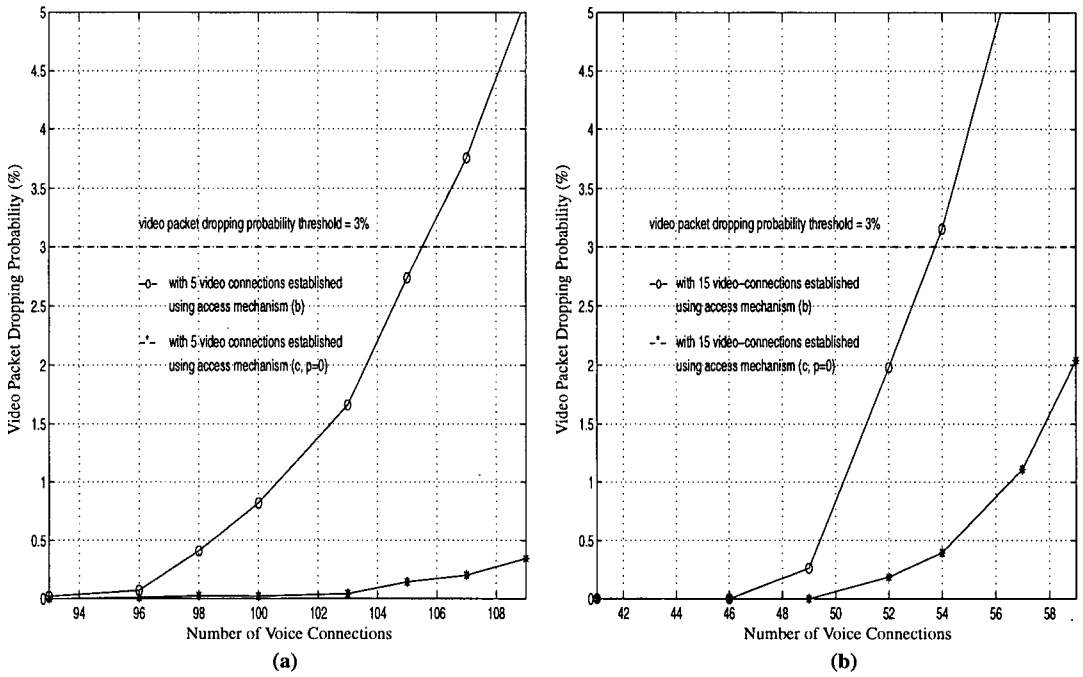

Figure 5.13. Packet Dropping Probability of Video Traffic When Access Mechanism (c, p=0) is Applied.

Figure 5.12 shows that, when access mechanism (c, p=0) is used, the 5-percentile access delay experienced by the video traffic is reduced when compared to the system using access mechanism (b) under the same traffic-load condition. Moreover, when access mechanism (c, p=0) is used, the increase in access delay of the video traffic is less sensitive to the increase in voice traffic level. These results are expected because, when access mechanism (c, p=0) is used, the access delay of the video traffic is not affected by the number of voice terminals waiting in the low priority I-slot allocation queue. However, as observed in Figure 5.12, as the voice traffic level further increases, the video traffic still experience an increase in access delay. It is because when a reservation request from a video terminal arrives, if there is no free I-slot available, the video terminal may need to wait for the lower priority voice terminals (that have been allocated with I-slots before the arrival of the video terminal) to finish their transmissions.

Figure 5.13 shows that the video packet dropping probability is reduced when access mechanism (c, p=0) is used. Since the video traffic experience a lower access delay when it has a higher priority in accessing channels, the probability that a video packet violates the 10 ms access delay threshold is reduced; as such, the video packet dropping probability decreases accordingly.

Figures 5.14 and 5.15 show the effects of using access mechanism (c, p=0) on the QoS of the voice traffic when there are 5 and 15 video-connections established.

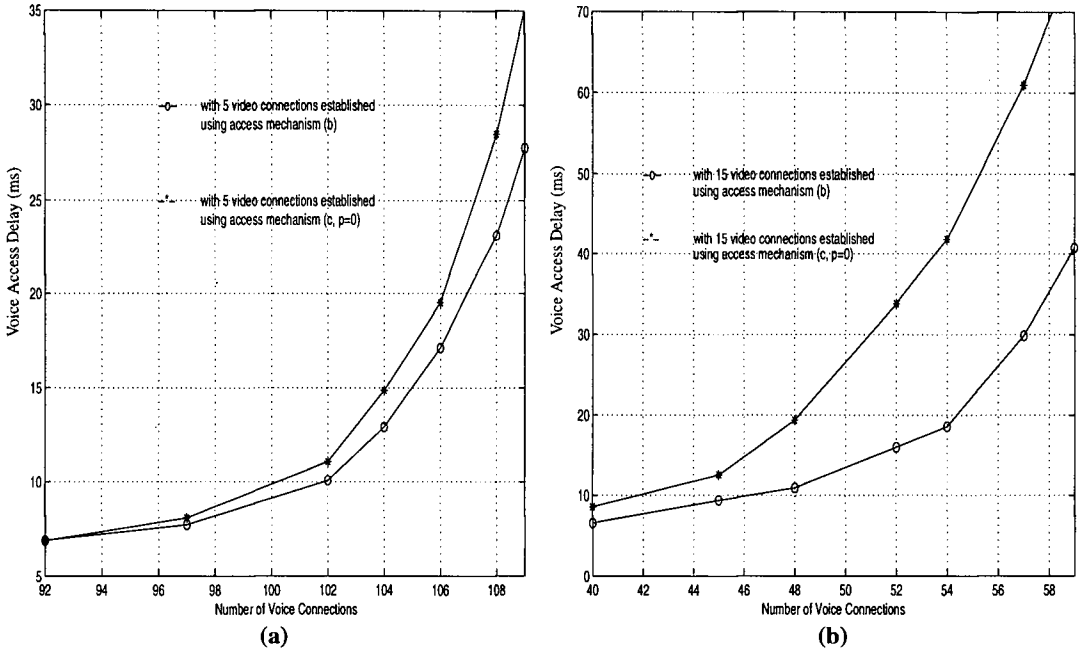

Figure 5.14. Access Delay of Voice Traffic When Access Mechanism (c, p = 0) is Applied.

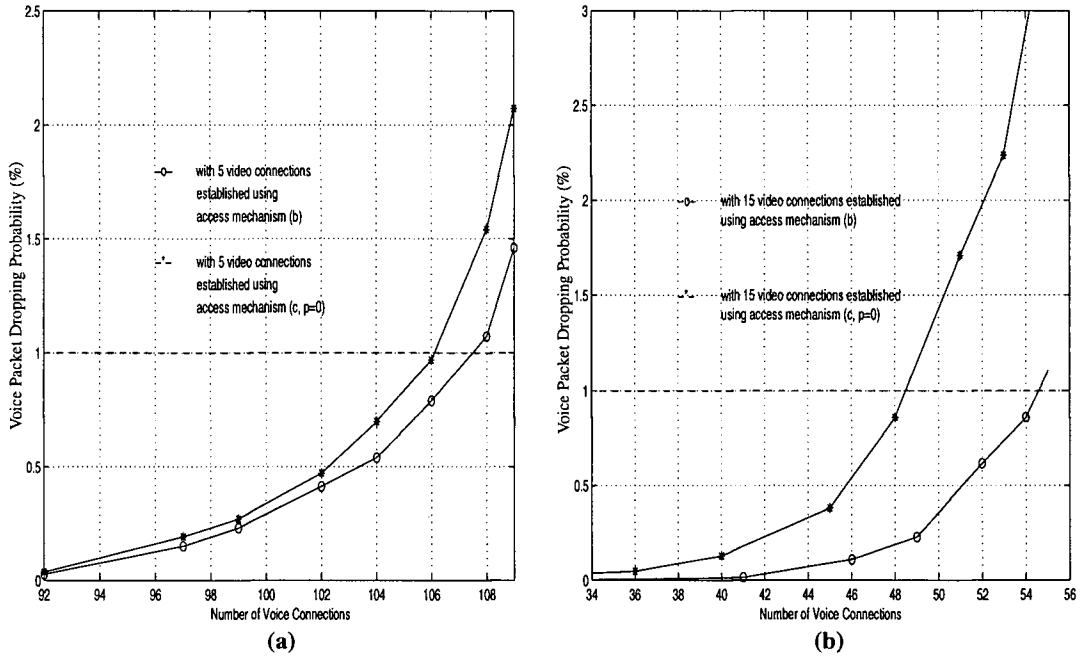

Figure 5.15. Packet Dropping Operability of Voice Traffic when Access Mechanism (c, p=0) is

Figure 5.14 shows that when access mechanism (c, p=0) is used, the access delay of the voice traffic is higher when compared to the system using access mechanism (b). In access mechanism (c, p=0), the voice traffic suffers an additional queueing delay because reservation requests from video terminals may arrive while the voice terminals are waiting in the low priority queue; therefore, voice terminals will stay longer in queue since they will only be served when all requests from video terminals are satisfied. Furthermore, as the number of video connections established in the system increases, the additional queueing delay of the voice traffic is further increased because the higher arrival rate of reservation requests from video terminals may result in the arrival of more video requests while a voice terminal is waiting in queue. This is seen in Figure 5.14: as the number of video connections established in the system increases from 5 to 15, the difference in voice traffic access delay between the systems using the two access mechanisms increases. Figure 5.15 shows the packet dropping probability of the voice traffic when there are 5 and 15 video-connections established. In access mechanism (c, p=0), the voice traffic, which has lower priority in accessing channel, experience a higher access delay; therefore, more packets need to be dropped because they violate the 10 ms access delay limit. By applying the 1% voice packet dropping probability as a threshold, a maximum of 106 and 48 voice connections can be established when there are 5 and 15 video connections in the system, respectively.

By establishing different numbers of video connections in the ATDMA system and analyzing the QoS of the voice and video services when access mechanism (c, p=0) is used, the acceptable traffic-load curve can be obtained as shown in Figure 5.16.

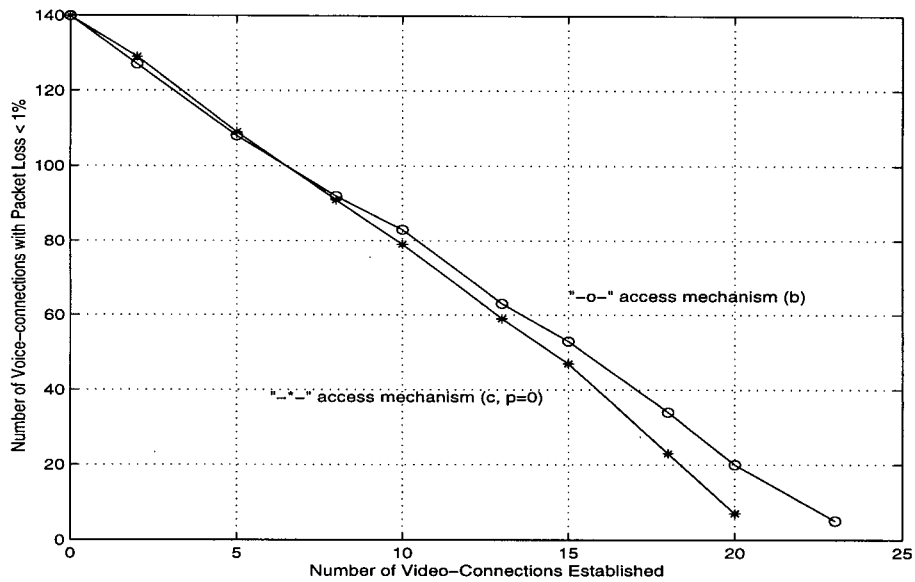

Figure 5.16. Acceptable Traffic-load Curves for Access Mechanisms (b) and (c, p=0)

Figure 5.16 shows that when the number of video connections established is below 6, the access mechanism (c, p=0) can increase the voice traffic capacity slightly. However, as the number of video connections increases further, access mechanism (c, p=0) causes too much quality degradation to the voice traffic. As a result, the capacity of the voice traffic is decreased as j increases (for $j > 6$). This observation suggests that when there is a low level of video traffic, a small "p" value can increase the system capacity because the improvement in QoS of the video traffic causes only a slight degradation in the quality of the voice traffic. However, as the level of video traffic increases, the video traffic causes a larger degree of quality degradation to the voice traffic. Therefore, a larger "p" value is more suitable for access mechanism (c, p) so that a larger portion of the voice traffic reservation requests is allowed to enter the high priority I-slot allocation queue. Thereby, the extent of the voice quality degradation caused by the presence of the video traffic can be reduced. Table 5.2 shows the effects of using higher "p" values for the access

mechanism (c, p) on the capacity of the ATDMA system under three different levels of video traffic.

Table 5.2 Effects of Using Different p Values in Access Mechanism (c, p)

(p)	5 video connections established				10 video connections established				15 video connections established			
	$N_c(5)$	P_{vo} (%)	P_{vi} (%)	D_{vi} (ms)	$N_c(10)$	P_{vo} (%)	P_{vi} (%)	D_{vi} (ms)	$N_c(15)$	P_{vo} (%)	P_{vi} (%)	D_{vi} (ms)
0	106	0.97	0.19	18.2	81	0.93	0.16	16.7	48	0.87	0.08	15.8
0.50	106	0.88	1.39	43.8	82	0.86	0.92	34.9	51	0.91	0.53	27.2
0.70	107	0.96	2.87	74.5	83	0.93	1.61	52.1	52	0.86	1.16	36.3
0.80	106	0.84	2.62	67.5	84	0.95	2.81	71.4	53	0.89	2.19	54.8
0.85	106	0.82	2.82	72.5	83	0.81	2.33	65.3	54	0.94	2.81	74.5
1	105	0.67	2.74	68.2	83	0.72	2.43	69.7	53	0.76	2.61	70.2

In Table 5.2, $N_C(j)$ denotes the maximum number of voice connections that can be accommodated together with j video connections (while the QoS thresholds for voice and video services are respected, simultaneously) when access mechanism (c) is used. It should be noted that when the probability "p" equal to 1, there is no priority difference between the voice and video services in accessing channels; thus, access mechanism (c, p=1) is equivalent to access mechanism (b). From Table 5.2, it is observed that, by choosing suitable "p" values under different video traffic-load conditions, access mechanism (c) can support a slightly higher voice-traffic capacity when compared to access mechanism (b). In general, a lower value of "p" can be used when there is a low level of video traffic. As the number of video connections established increases, a higher value of "p" should be used so that the QoS improvement achieved in video traffic will only cause a limited quality degradation to the voice traffic. For instance, when there are 5 video connections established, the voice traffic capacity can be increased from 105 connec-

tions (when access mechanism (b) is used) to 107 connections when a "p" value of 0.7 is used in access mechanism (c). However, when the number of video connections is increased to 15, a higher value of "p" equal to 0.85 is needed to increase the voice-traffic capacity from 53 (as obtained using access mechanism (b)) to 54 connections.

Chapter 6 Conclusions

To meet the anticipated demand for multimedia services in cellular systems, a modified access mechanism (based on the PRMA++ access method used in the ATDMA project) which allows the base station to dynamically assign channels to different types of traffic based on their transmission bit-rate requirements has been proposed. The performance of the modified access mechanism is studied through extensive computer simulations in three areas. First, we examined the efficiency of the modified access mechanism in supporting video service only in the ATDMA system. Next, we studied the performance when both voice and video services are supported in the system. Finally, we examined the effects of assigning different priorities to the voice and video services in accessing channels. The QoS threshold for the voice service is 1% packet dropping probability. For the video service, the QoS thresholds are a 5-percentile access delay of 76.7 ms and a packet dropping probability of 3%.

6.1 Summary and Findings

The video traffic considered in this thesis is low-resolution video which can be used in videophone applications. The output bit-rate of the video coder depends on the complexity of the video frame being encoded and on the movement of objects in front of the cameras. A Markov chain model with three states is used to model the output bit-rate of the video traffic. The maximum bit-rate of a video coder can be supported in the ATDMA system by using 4 time-slots per transmission frame while the minimum bit-rate of the video coder requires 2 time-slots per transmission frame. The modified access mechanism allows the base station to allocate I-slots to video terminals according to their output bit-rate. During low activity periods of video terminals, surplus time-slots are released back to the base station so that the time-slots can be re-allocated to

other terminals experiencing high activity periods. Simulation results show that for a 72 time-slot ATDMA system, the modified access mechanism can support a maximum number of 26 video connections (5-percentile access delay is 62 ms and packet dropping probability is 2.5%), when 1 R-slot and 1 A-slot are used on the up-link and down-link to serve as control channels respectively. As a comparison, the access method used in the ATDMA project can support a maximum of 18 video connections.

When voice and video services are supported simultaneously in the ATDMA system and have the same priority in accessing channels, simulation results show that the modified access mechanism can support a higher traffic load when compared to the access method used in the ATDMA project. In the modified access mechanism, the base station assigns I-slots to video terminals based on their bit-rate activities. In contrast, the access mechamism used in the ATDMA system assigns a fixed number of I-slots (4 I-slots) to a video connection during its period of activity. As a result, under the same video traffic-load condition, the dynamic I-slot allocation strategy used in the modified access mechanism allows the base station to maintain a larger number of free I-slots which can be used to support more voice mobiles in the system.

When voice and video have the same priority in accessing channels, simulation results show that the QoS thresholds of video traffic are reached before that of the voice traffic as traffic-load increases. A simple priority scheme is proposed which, under different traffic-load conditions, can assign an adjustable priority (controlled by the parameter "p") to the video service over the voice service. In the priority scheme, a smaller "p" value corresponds to a higher priority for the video service. Simulation results show that, in general, a lower "p" value can be used to increase the system capacity when there is a low level of video traffic. As the number of video

connections increases, a larger "p" value should be chosen so that the QoS improvement achieved in the video traffic does not result in a large QoS degradation for the voice traffic.

6.2 Topics for Future Investigation

So far, the video source model used in this thesis has not been verified using statistics from low bit-rate video codecs such as the H.263 codec [25] and the MPEG4 [28]. Such a verification will be needed to confirm the performance results presented. Furthermore, error-free links were assumed. The effect of channel errors on the capacity of the ATDMA system using the modified access mechanism is another topic to be studied.

Data services (such as e-mail, facsimile and compressed image transfer), which do not tolerate information loss but can accept a relatively high access delay when compared to real-time voice and video services, can also be supported in the ATDMA system using the modified access mechanism. Possible topics for further research include:

- Capacity determination of the ATDMA system when voice, video and data services are supported simultaneously using the modified access mechanism.
- Determination of a suitable priority scheme which allows the base station to maximize the system capacity by prioritizing the I-slot allocations to different service types based on their QoS thresholds.

Moreover, the problems associated with handoff calls can be investigated as an extension of this thesis. Handoff is time-critical since it ensures the continuity of a call. In order to reduce the handoff blockage probability, there is a need to choose a priority scheme which favors the handoff calls in accessing channels while limiting the quality degradation suffered by other

mobiles in the cell.

Glossary

This section provides a list of acronyms and abbreviations used in this thesis.

B-ISDN	-Broadband - Integrated Services Digital Network
DCT	-Discrete Cosine Transform
DECT	-Digital European Cordless Telecommunications
EIA	-Electronic Industries Association (U.S.)
FEC	-Forward Error Correction
GSM	-Global System for Mobile Communication
IEC	-International Electrotechnical Comission
IS-54	-Interim Standard 54 (TIA/EIA TDMA cellular Standard, U.S.)
ISO	-International Standards Organization
ITU-T	-International Telecommunications Union
MAC	-Medium Access Control
MPEG	-Motion Picture Expert's Group
PCS	-Personal Communication Systems
PHS	-Personal Handyphone System
PRMA	-Packet Reservation Multiple Access
QoS	-Quality of Service
RACE	-R&D in Advanced Communication Technologies in Europe
TDMA	-Time Division Multiple Access
TIA	-Telecommunications Industry Association (U.S.)
UMTS	-Universal Mobile Telecommunications System
VAD	-Voice Activity Detector

Bibliography

[1] D.D. Falconer, F. Adachi, and B. Gudmundson, "Time Division Multiple Access Methods for Wireless Personal Communications," *IEEE Communications Magazine,* vol. 33, no.1, pp. 50-57, January 1995.

[2] R. Beraldi, A. Iera, S. Marano, and P. Salerno, "A New Dynamic Reservation Multiple Access Protocol for Supporting Multimedia Traffic in a Third Generation Cellular System," *Proceedings of IEEE ICC '94*, Singapore, pp. 314 - 319, November 1994.

[3] J.E. Padgett, C. G. Gunther and T. Hattori, "Overview of Wireless Personal Communications," *IEEE Communications Magazine*, pp. 28 - 41, January 1995.

[4] D. Raychaudhuri and N. Wilson, "Multimedia Transport in Next-Generation Personal Communication Networks," *Proceedings of IEEE ICC '93*, Geneva, Switzerland, pp. 858 - 862, May 1993.

[5] J. Dunlop, J. Irvine, D. Robertson, and P. Cosimini, "Performance of a statistically Multiplexed Access Mechanism for a TDMA Radio Interface," *IEEE Personal Communications*, vol. 2, no. 3, pp. 56 - 64, June 1995.

[6] J. Dunlop, P.Cosimini, D. Maclean, D. Robertson, and D. Aitken, "A Reservation Based Access Mechanism for 3rd Generation Cellular Systems," *IEE Electronics and Communication Engineering Journal,* vol. 5, no. 3, pp. 180 - 186, June 1993.

[7] J. M. Devile, "A Reservation Based Multiple Access Scheme for a Future Universal Mobile Telecommunications System," *IEE European Conference on Mobile and Personal Communications*, London, UK, pp. 210 - 215, December 1993.

[8] D. J. Goodman and S. X. Wei, "Efficiency of Packet Reservation Multiple Access," *IEEE Transactions on Vechicular Technology*, vol. 40, no. 1, pp. 170 - 176, February 1991.

[9] A. Urie, M. Streeton, and C. Mourot, "An Advanced TDMA Mobile Access System for UMTS," *IEEE Personal Communications*, vol. 2, no. 1, pp. 38 - 47, February 1995.

[10] K. Nahrstedt and R. Steinmetz, "Resource Management in Networked Multimedia Systems," *Computer*, vol. 28, no. 5, pp. 52 - 63, May 1995.

[11] J.G. Proakis, *Digital Communications*. McGraw-Hill, 3rd Edition, 1995. ISBN 0-07-051726-6.

[12] J. Dunlop, P. Cosimini, and D. Robertson, "Optimization of Packet Access Mechanisms for Advanced Time Division Multiple Access ATDMA," *IEE European Conference on Mobile and Personal Communications*, London, UK, pp. 237 - 242, December 1993

[13] A. Kamas, et al., *Ptolemy: The Almagest - Vol. I-IV.* University of California at Berkeley, Berkeley, CA, 0.5.2 Edition, May 1995.

[14] F. Li and L. F. Merakos, "Voice/ Data Channel Access Integration in TDMA Digital Cellular Networks," *IEEE Transactions on Vechicular Technology*, vol. 43, no. 4, pp. 986 - 996, November 1994.

[15] M. Woo, N. Prabhu, and A. Ghafoor, "Dynamic Resource Allocation for Multimedia Services in Mobile Communication Environments," *IEEE Journal on Selected Areas in Communications*, vol. 13, no. 5, pp. 913 - 922, June 1995.

[16] R. R. Gejji, "Mobile Multimedia Scenario Using ATM and Microcellular Technologies," *IEEE Transactions on Vechicular Technology*, vol. 43, no. 3, pp. 699 - 703, August 1994.

[17] ITU-T Recommendation H.261, "Video Codec for audio-visual services at px64kbits/s," 1992.

[18] K. Sayood, *Introduction to Data Compression*. San Francisco: Morgan Kaufmann, 1996.

[19] Ming Liou, "Overview of the px64 kbits/s Video Coding Standard," *Communications of the ACM*, vol. 34, no. 4, pp. 59-63, April 1991.

[20] H. Liu and M. E. Zarki, "Transmission of video telephony images over wireless channels," *ACM Wireless Networks*, vol. 2, no. 1, pp. 219 - 228, January 1996.

[21] M. Conti and E. Gregori, "Analysis of Bandwidth Allocation Schemes for Transmission of VBR Video Traffic on a FODA Satellite Network," *IEE Proceedings on Communications,* vol. 143, no. 1, pp. 12 - 20, February 1996.

[22] H. Heeke, "A Traffic-Control Algorithm for ATM Networks," *IEEE Transactions on Circuits and Systems for Video Technology*, vol. 3, no. 3, June 1993.

[23] D. Bertsekas and R. Gallager, *Data Networks*. New Jersey: Prentice-Hall Inc., 2nd Edition, 1992.

[24] ITU-T/ SG15, Draft Recommendation H.263, "Video coding for low bit-rate communication (1995)".

[25] M. W. Whybray and W. Ellis, "H.263 - Video Coding Recommendation for PSTN Videophone and Multimedia," *IEE Colloqium on Low Bit Image Coding*, London, UK, pp. 6/1 - 6/9, June 1995.

[26] P. Cherriman and L. Hanzo, "Robust H.263 Video Transmission Over Mobile Channels in Interference Limited Environment," *IEE Proceedings on Communications*, vol. 146, no. 2, pp. 22 - 35, February 1996.

[27] R. Steinmetz, "Human Perception of Jitter and Media Synchronization," *IEEE Journal on Selected Areas in Communications*, vol. 14, no. 1, January 1996.

[28] T. Sikora, "MPEG-4 Very Low Bit Rate Video," *Proc. IEEE ISCAS Conference,* Hong Kong, June 1997.